Oil & Natural Gas Technology

DOE Award No.: DE-FE0013590

Final Scientific/Technical Report

TA [2] Continuous, regional methane emissions estimates in northern Pennsylvania gas fields using atmospheric inversions

Project Period (10/01/2013 to 05/31/2017)

Submitted by:
PI Thomas Lauvaux

_____ _____December 2017_____
Signature Submission date

Recipient address:
The Pennsylvania State University
DUNS #:00-340-3953.
110 Technology Center building
University Park, PA 16802
e-mail: tul5@psu.edu
Phone number: (814) 863-4321

Prepared for:
United States Department of Energy
National Energy Technology Laboratory

Office of Fossil Energy

DISCLAIMER

ABSTRACT

Natural Gas (NG) production activities in the northeastern Marcellus shale have significantly increased in the last decade, possibly releasing large amount of methane (CH_4) into the atmosphere from the operations at the production sites and during the processing and transmission steps of the natural gas chain. Based on an intensive aircraft survey, leakage rates from the NG production were quantified in May 2015 and found to be in the order of 0.5% of the total production, higher than reported by the Environmental Protection Agency (EPA) but below the usually observed leakage rates over shale gases in the US. Thanks to the high production rates on average at each well, leakage rates normalized by production appeared to be low in the northeastern Marcellus shale. This result confirms that natural gas production using unconventional techniques in this region is emitting relatively less CH_4 into the atmosphere than other shale reservoirs. The low emission rate can be explained in part by the high productivity of wells drilled across the northeastern Marcellus region. We demonstrated here that atmospheric monitoring techniques can provide an independent quantification of NG leakage rates using aircraft measurements. The CH_4 analyzers were successfully calibrated at four sites across the region, measuring continuously the atmospheric CH_4 mixing ratios and isotopic $^{13}CH_4$. Our preliminary findings confirm the low leakage rates from tower data collected over September 2015 to November 2016 compared to the aircraft mass-balance estimates in May 2015. However, several episodes revealing large releases of natural gas over several weeks showed that temporal variations in the emissions of CH_4 may increase the actual leakage rate over longer time periods.

TABLE OF CONTENTS

EXECUTIVE SUMMARY

Natural gas infrastructure releases methane (CH_4), a potent greenhouse gas, into the atmosphere. The estimated emission rate associated with the production and transportation of natural gas is uncertain, hindering our understanding of its greenhouse footprint. During the project, a new application of inverse methodology was developed for estimating regional emission rates from natural gas production and gathering facilities in north-eastern Pennsylvania. An inventory of CH_4 emissions was compiled for major sources in Pennsylvania. This inventory served as input emission data for the Weather Research and Forecasting model with chemistry enabled (WRF-Chem), and atmospheric CH_4 mole fraction fields were generated at 3km resolution. Simulated atmospheric CH_4 enhancements from WRF-Chem were compared to observations obtained from a 3-week flight campaign in May 2015. Modelled enhancements from sources not associated with upstream natural gas processes were assumed constant and known and therefore removed from the optimization procedure, creating a set of observed enhancements from natural gas only. Simulated emission rates from unconventional production were then adjusted to minimize the mismatch between aircraft observations and model-simulated mole fractions for 10 flights. To evaluate the method, an aircraft mass balance calculation was performed for four flights where conditions permitted its use. Using the model optimization approach, the weighted mean emission rate from unconventional natural gas production and gathering facilities in north-eastern Pennsylvania approach is found to be 0.36 % of total gas production, with a 2σ confidence interval between 0.27 and 0.45 % of production. Similarly, the mean emission estimates using the aircraft mass balance approach are calculated to be 0.40 % of regional natural gas production, with a 2σ confidence interval between 0.08 and 0.72 % of production. These emission rates as a percent of production are lower than rates found in any other basin using a top-down methodology, and may be indicative of some characteristics of the basin that make sources from the north-eastern Marcellus region unique.

During the second part of the project, four in-situ cavity ring-down spectrometers (G2132-i, Picarro, Inc.) measuring methane dry mole fraction (CH_4), carbon dioxide dry mole fraction (CO_2) and the isotopic ratio of methane ($\delta^{13}CH_4$) were deployed at four towers in the Marcellus Shale natural gas extraction region of Pennsylvania. The calibration of the continuous isotopic methane analyzers used in this project required both a linear calibration and a mole fraction correction, and a correction for cross-interference from ethane. Laboratory and field calibration of the analyzers was needed for tower-based applications, and to characterize their performance in the field for the period January–December 2016. Prior to deployment, each analyzer was calibrated using high methane mole fraction air bottles with various isotopic ratios, from biogenic to thermogenic source values, diluted in zero air. Furthermore, at each tower location, three field calibration tanks were employed, from ambient to high mole fractions, with various isotopic ratios. By testing multiple calibration schemes, we determined an optimized field calibration method. A method to correct for cross interference from ethane is also described. Using an independent field tank for evaluation, the standard deviation of 4-hour means of the isotopic ratio of methane difference from the known value was found to be 0.26 ‰ δ13CH4. Following improvements in the field calibration tank sampling scheme, the standard deviation of 4-hour means was 0.11 ‰, well within the target compatibility of 0.2 ‰. Round robin style testing using tanks with near ambient isotopic ratios indicated mean errors of −0.14 to 0.03 ‰ for each of the analyzers. Flask to in-situ comparisons showed mean differences over the year of 0.02 and 0.08 ‰, for the East and South towers, respectively.

Regional sources in this region were difficult to differentiate from strong perturbations in the background. During the afternoon hours, the median enhancements of isotopic ratio measured at three of the towers, compared to the background tower, were −0.15 to 0.12 ‰ with standard deviations of the 10-min isotopic ratio enhancements of 0.8 ‰. In terms of source attribution, analyzer compatibility of 0.2 ‰ δ13CH4 affords the ability to distinguish a 50 ppb CH4 peak from a biogenic source from one originating from a thermogenic source.

Using a Keeling plot approach for the non-afternoon data at a tower in the center of the study region, we determined the source isotopic signature to be −31.2 ‰, consistent with a deep-layer Marcellus natural gas source.

In the last phase of the project, the atmospheric CH_4 mixing ratios collected over the 18 months (September 2015 - March 2017) were analyzed to identify temporal and spatial variability in the sources of CH_4. The first analysis was performed using the smoothed mixing ratios of the downwind sites, after removing the background conditions defined at the upwind locations. The results show large variations in the strength of the emissions from the northeastern Marcellus, enhanced for several weeks during multiple events over the two years of the deployment. The signals in atmospheric measurements suggest that operations related to the production or the transmission of the natural gas produce large amount of CH_4 over short periods of time, which therefore require long-term monitoring in order to quantify these variations in leakage rates. The second analysis uses a full Bayesian inversion system constructed around the WRF mesoscale model and a Lagrangian Particle Dispersion Model (LPDM), and spatially-defined CH_4 emissions at 1km resolution. Inverse emissions have been computed for October to December 2015, indicating similar leakage rates over the northeastern Marcellus shale (about 0.5% or less). Further analysis of the data is ongoing and will be published in the coming months after completion of the inversion over the deployment period.

Team members:

PennState Meteorology
Thomas Lauvaux: Principal Investigator, Modeling Analysis
Natasha L. Miles: Data analysis, Calibration protocol
Scott L. Richardson: Instrument deployment, Instrument design
Ken J. Davis: Aircraft campaign, Data analysis
Zachary Barkley: Modeling Analysis, Emission Optimization
Aijun Deng: Modeling analysis, Aircraft forecast

PennState Marcellus Center (MCOR)
Tom Murphy: Inventory preparation, Observing strategy

NOAA / CIRES
Colm Sweeney: Aircraft campaign, Data analysis
Anna Karion: Aircraft campaign, Automated flask sampling
Kathryn McKain: Data analysis, Automated flask sampling

Picarro, Inc.
Chris Rella: Drive-around analysis, Instrument development

REPORT DETAILS

Comparison of the actual accomplishments with the goals and objectives of the project

The objective of this project was to quantify fugitive emissions of CH_4 from the Marcellus gas production region of north-central Pennsylvania over a period of two years, with weekly temporal resolution and 10 km^2 spatial resolution using atmospheric inversion technology. These regional gas production emissions estimates are to be accompanied by estimates of total CH_4 emissions, and a break down of the relative contribution of various regional sources (animal agriculture, wetlands, landfills, gas production, other regional sources identified) to the regional total. Regional source attribution are to be obtained primarily by analyses of the chemical signatures of these sources. Additionally, atmospheric inversion estimates were to be compared to emissions-factor, activity-data based "inventory" regional CH4 emissions estimates, evaluating both the accuracy of the inventory methods, and our ability to detect changes over time in emissions caused by changing gas production activity.

The main objective and the following sub-tasks have been successfully accomplished during the course of the project. The emissions have been computed using aircraft measurements (Barkley et al., 2017). Atmospheric mixing ratios of CH_4 and $^{13}CH_4$ have been collected at high accuracy by implementing a robust calibration protocol (Miles et al., 2017). The source attribution in the northeastern region of the Marcellus shale was also performed using our modeling approach (WRF coupled to EPA components of the inventories) and by considering and $^{13}CH_4$ hydrocarbons. The last part of the project, i.e. comparison of the emissions to activity data over 18 months in the Marcellus shale, revealed multiple time periods with high atmospheric enhancements which remains unexplained using reported activity data in the region. These large atmospheric enhancements measured during the project period may highlight unreported CH_4 releases from natural gas production activities. Future projects need to address these unreported events which may explain the higher leakage rate observed here compared to EPA. From these activities, two additional studies are about to be published, the first one with University of Maryland using the same WRF modeling systems to analyze an aircraft campaign in southwestern Pennsylvania (Ren et al., in prep.), and a second to compare the updated inventory prepared by the Environmental Defense Fund (Alavarez et al., in prep.).

Summary of project activities for the entire period of funding

The results of the project and the links to archived data are presented in the following website: http://sites.psu.edu/marcellus/. This website will be maintained and updated by the research group at The Pennsylvania State University.

Task 1 Project Management and Planning

The Project Management and Planning was submitted within 30 days of the award.

Task 2 Construction of prior estimates of CH_4 emissions in the northern Marcellus region

Subtask 2.1 Collection of activity data for the preparation of a bottom-up CH_4 emission map , including biogenic and thermogenic sources

In this project, we characterized emissions from the natural gas industry into five different sectors: emissions from wells, emissions from compressor facilities, emissions from storage facilities, emissions from pipelines, and emissions in the distribution sector. To estimate CH_4 emissions from the production sector of the natural gas industry, data were first obtained on the location and production rate of each unconventional well from the Pennsylvania Department of Environmental Protection Oil and Gas Reports website (PADEP, 2016) and the West Virginia Department of Environmental Protection (WVDEP, 2016). To convert the production rate into an emission rate, we need to assume a first guess as to the expected leakage from wells in the area. A first-guess natural gas emission rate of 0.13 % was applied to the production value of each of the 7000+ producing unconventional wells based on the median rate from Omara et al. (2016). The natural gas emission rate was then converted to a CH4 emission rate by assuming a CH4 composition in the natural gas of 95 % (Peischl et al., 2015).

In addition to unconventional wells, the domain also contains more than 100,000 shallow conventional wells. Annual conventional production rates for the year 2014 were obtained through the PA DEP Oil and Gas Reports website, the WV DEP, and the New York Department of Environmental Conservation (NY DEC, 2016). Despite the large number of wells, the average conventional well in PA produces 1 % of the natural gas of its unconventional counterpart. However, it is speculated that the older age of these wells and a lack of maintenance and care for them results in a higher emission rate for these wells as a function of their production (Omara et al., 2016). A first-guess natural gas emission rate of 11 % was applied to the production values of the conventional wells based on the median emission rate from the wells sampled in Omara et al. (2016). Similarly to the unconventional wells, the natural gas emission rate was then converted to a CH4 emission rate by assuming a CH4 composition in the natural gas of 95 %.

Compressor stations located within the basin are responsible for collecting natural gas from multiple well locations, removing non-CH_4 hydrocarbons and other liquids from the flow, and regulating pressure to keep gas flowing along gathering and transmission pipelines, and can be a potential source for methane emissions. Data for compressor station locations and emissions come from a data set used in Marchese et al. (2015). A total of 489 compressor facilities are listed for Pennsylvania, with 87 % of the listed facilities also containing location data. Emissions for each compressor station are calculated through two different methodologies. In the simplest case, a flat emission rate of 32.35 kg h−1 is applied to each station, which is the mean emission rate of a gathering facility in PA found in Marchese et al. (2015). In the more complex scenario, the same emissions total is used as in the flat rate case but is distributed among the compressor stations linearly as a function of their energy usage. Wattage between compressors in our data set can vary greatly, from 10 kW for small compressors to 7000 kW or more at large gathering facilities. Using the wattage as a proxy for emissions allows us to account for the size and throughput of natural gas at each station and assumes larger stations will emit more natural gas compared to smaller stations (Marchese et al., 2015). Data on locations of underground storage facilities were obtained from the United States Energy Information Administration (EIA, 2015). For each of these locations, a base emission rate of 96.7 kg h−1 was applied according to the average value emitted by a compressor station associated with an underground storage facility (Zimmerle et al., 2015).

To calculate pipeline emissions, data on pipeline locations needed to be collected. Information on transmission pipelines, which connect gathering compressors to distribution networks, is provided by the Natural Gas Pipelines GIS product purchased from Platts, a private organization which collects and creates various infrastructural layers for the natural gas and oil industry (Platts, 2016). Gathering pipeline data corresponding to the transfer of gas from wellheads to gathering compressors is nearly non-existent for PA with the exception of Bradford County (2016), which maps out all gathering pipeline infrastructure within the county border. In PA, information on the location of a gathering pipeline elsewhere is only available where a gathering line crosses a stream or river. To account for gathering pipelines in the remainder of the state, a GIS model was

created using Bradford County pipelines maps in addition to previously generated pipeline maps of Lycoming County (Langlois et al., 2017). A typical pattern was simulated, connecting pipelines between unconventional wells throughout the state. The resulting pattern follows the valley of the Appalachian Mountains, with larger pipelines crossing through the state to connect the different branches of the network. These pipelines were then multiplied by an emission factor of 0.043 kg per mile of pipe, used for gathering pipeline leaks in the Inventory of US Greenhouse Gas Emissions and Sinks: 1990–2013 (EPA, 2015b).

CH_4 emissions from natural gas distribution sources, coal mines, and animals/animal waste were provided from Maasakkers et al. (2016), which takes national-scale emissions from the EPA's greenhouse gas inventory for the year 2012 and transforms it into a $0.1^\circ \times 0.1^\circ$ emissions map for the continental USA. For natural gas distribution emissions, various pipeline data were collected at state level and emission factors were accounted for to calculate a total distribution emission for the state. This emissions total was then distributed within the state, proportional to the population density. Emission estimates for coal are calculated using information from the Greenhouse Gas Reporting Program (GHGRP) for active mines and the Abandoned Coal Mine Methane Opportunities Database for abandoned mines (EPA, 2008). State-level emissions missions from enteric fermentation and manure management are provided in the EPA's inventory. These emissions were segregated into higher resolutions using county-level data from the 2012 US Census of Agriculture (USDA, 2012) and land-type mapping.

Finally, the EPA's Greenhouse Gas Reporting Program data set for the year 2014 was used to capture all other major sources of CH_4 in the region that are otherwise unaccounted for, the majority of which are emissions from landfills and some industrial sources (EPA, 2015a). Sources within the GHGRP that overlap with natural gas sources already accounted for within our inventory were removed to prevent redundancy. Although our emissions map used for the model runs did not account for potential CH_4 emissions from wetland sources, a series of wetlands emission scenarios was obtained for the region using data from Bloom et al. (2017). From this data set, wetland CH4 emissions make up only 1 % of all regional CH_4 emissions in the most extreme scenario, and thus we assume their impact is negligible in this study.

Subtask 2.2 Collection of field data to evaluate prior CH_4 emission estimates and partition source contributions

Chris Rella from Picarro, Inc., joined for a one week campaign in northeastern Pennsylvania. The equipment brought by Rella included the $^{13}CH_4$ CRDS analyzer, calibration gases, a low flow air pump, and the MegaCore (long tube of 3,000ft for the collection of air during the drive around). Rella provided the design of the instrumentation for sampling the MegaCore with the control of the flow and the repeated calibration periods with multiple standards for CH_4 and $^{13}CH_4$.

A total of 3 drive-arounds took place over 2 weeks with a 1st drive aiming at measuring signals across the 3 counties in Pennsylvania, a 2nd drive to measure the background signals in the state of New York, and a 3rd drive in NE PA to sample different parts of the three counties. The three campaigns took place at night, when CH_4 concentrations were high (low wind speed) and the accumulation in the stable nocturnal planetary boundary layer was high. Several sources were identified including biogenic sources and thermogenic sources during multiple drive-arounds. Using a low flow air pump, the megacore offers a spatial resolution of about 5km. The results from the drive-around confirmed the a priori emission maps generated in the subtask 1.1. No major source has been detected during these campaigns.

Subtask 2.3 Network design based on prior CH_4 emissions and atmospheric modeling

Based on the location of the wells and other sources in the northeastern Marcellus, a set of four towers was defined to provide information on the background (upwind conditions) and about the natural gas production area (downwind sites). The design was based on model simulations to capture the maximum amplitude in the atmospheric mixing ratios, but also a clear background depending on the main wind directions. Four locations were selected, as shown in Figure 1. The initial search identified 18 existing infrastructures suitable for deployment. The selection of the sites was based on multiple criterias including the presence of sources in the vicinity (exclusion), the distance to the main sources compared to the climatological wind directions (from the West and the South), the tower heights, and the definition of the background air (upwind of the sources). After identifying the nearby sources for the 18 tower locations, we selected four locations with optimal characteristics. The towers were instrumented with Picarro CRDS CH_4/$^{13}CH_4$ sensors as described in the following section.

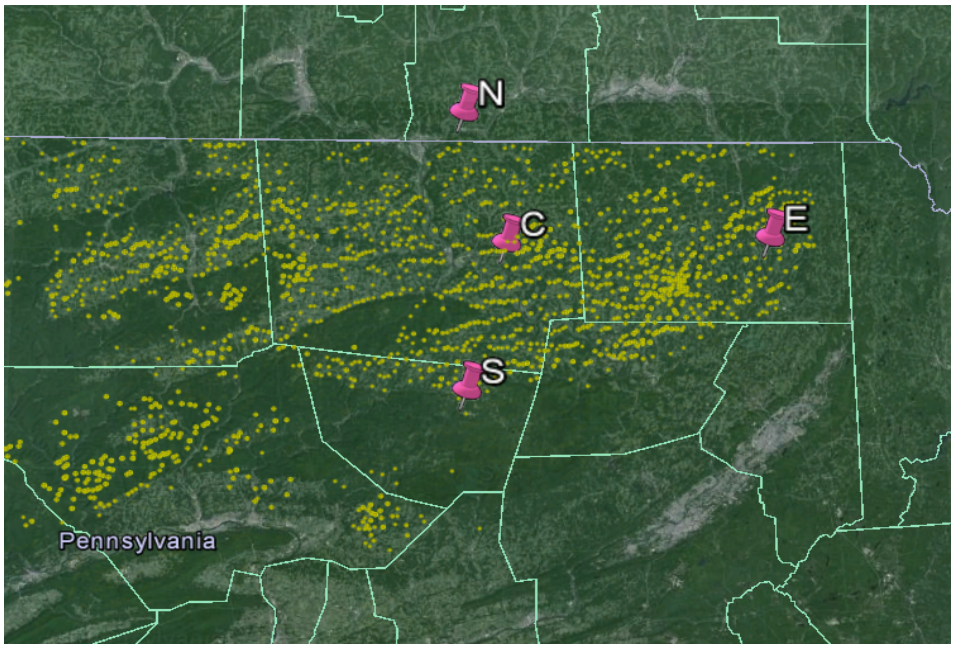

Figure 1: four tower locations instrumented during the project. The South tower (S) and North tower (N) provided background concentrations while Central (C) and East (E) towers measured the enhanced concentrations of CH_4 from the unconventional gas production area.

Task 3 Deployment of the surface tower network and configuration of the inversion system

Subtask 3.1 Deployment of calibrated CRDS instruments at the four identified tower locations

Picarro G2132-i analyzers were deployed in May 2015 at four communications towers, measuring methane concentrations continuously. Because boundary conditions are an absolute necessity to define the local enhancement, two towers out of four were dedicated to this task. At any given time, at least one of the two will be used to define the background conditions. In some specific wind conditions, both may be measuring the background. The two towers instrumented to measure methane concentrations in the predominantly downwind direction from the major source area are the towers Central (C) and East (E). As shown by the DEP production report, the most productive area is located between towers C and E, with a large number of recent wells. The other two towers (Towers North (N) and South (S)) measure alternatively the background concentrations or the enhanced concentrations depending on the wind direction. If the mean wind direction is from SW to SE angle, tower S is background and N is measuring potential emissions from the NE Marcellus

region. If the mean wind direction is from the NW to NE, tower N is upwind and S is downwind. In a pure westerly or easterly flow, both sites could be used to define the background conditions.

To calibrate the $\delta^{13}CH_4$ measurement prior to deployment, four different target mixing ratios, each at four different known isotopic ratios were sampled by the four analyzers using the experimental setup. Commercially-available isotopic standard bottles (Isometric Instruments, Inc., product numbers L-iso1, B-iso1, T-iso1 and H-iso1) were diluted with zero air to produce mixtures with varying CH_4 mixing ratios and $\delta^{13}CH_4$. The gravimetrically-determined zero air (Scott Marrin, Inc.) was natural ultra-pure air, containing no methane or other alkanes but ambient levels of CO_2. The isotopic calibration standard bottles each contained approximately 2500 ppm of CH_4 at –23.9, –38.3, –54.5, and –66.5 ‰ $\delta^{13}CH_4$, with uncertainty of ±0.2 ‰ reported by the supplier. Mass flow-controllers (MC-1SCCM and MC-500SCCM, Alicat Scientific, Inc.) and a 6-port rotary valve (EUTA-2SD6MWE, Valco Instruments Co., Inc.) were used to direct the standard bottle air for each isotopic calibration standard bottle into a mixing volume (~4 m of 1/8 in, 0.32 cm OD stainless steel tubing; TSS285-120F, VICI Precision Sampling, Inc.) at 0.400 sccm and mixed with zero CH_4 air at 137, 161, 303, and 555 sccm to create target CH_4 mole fractions of 7.3, 6.2, 3.3, and 1.8 ppm, respectively. Thus 16 CH_4 mole fraction/isotopic ratio pairs were produced. The accuracy of the mass flow controllers can be a significant source of error in making mixtures. Here the nominal range of the mass flow controllers was 1 sccm and 500 sccm, respectively, and the accuracy was ±0.2 % of full scale. To avoid isotopic fractionation at the head of the low-flow mass flow controller, the flow of the zero air was varied rather than the isotope standard. It is possible that fractionation did occur due to the tees used to direct gas into the individual analyzers. For this reason, it would have been preferable to set up the analyzers to sample from a common mixing volume.

A 3-way solenoid valve (091-0094-900, Parker Hannifin Corp.) was used just downstream of the mixing volume to stop flow from the zero air tank and Isometric Instrument bottles and allow flow from the working standards. In this way, the working standards were sequentially calibrated. The first mixture of each isotopic standard was sampled for 60 minutes to flush out the span gas line and to avoid isotopic fractionation at the head of the span mass flow controller. Subsequent dilutions using the same isotopic standard were sampled for 20 minutes each and each dilution was repeated twice. Observations were collected at ~0.5 Hz and the final 5 minutes of data for each dilution were averaged to compare against the target value. We note that these laboratory tests were completed prior to the Allan standard deviation testing and that the averaging times were not sufficient to achieve the desired compatibility for all but the highest mole fractions. Thus only the highest mole fractions are used for the linear calibration of the analyzers.

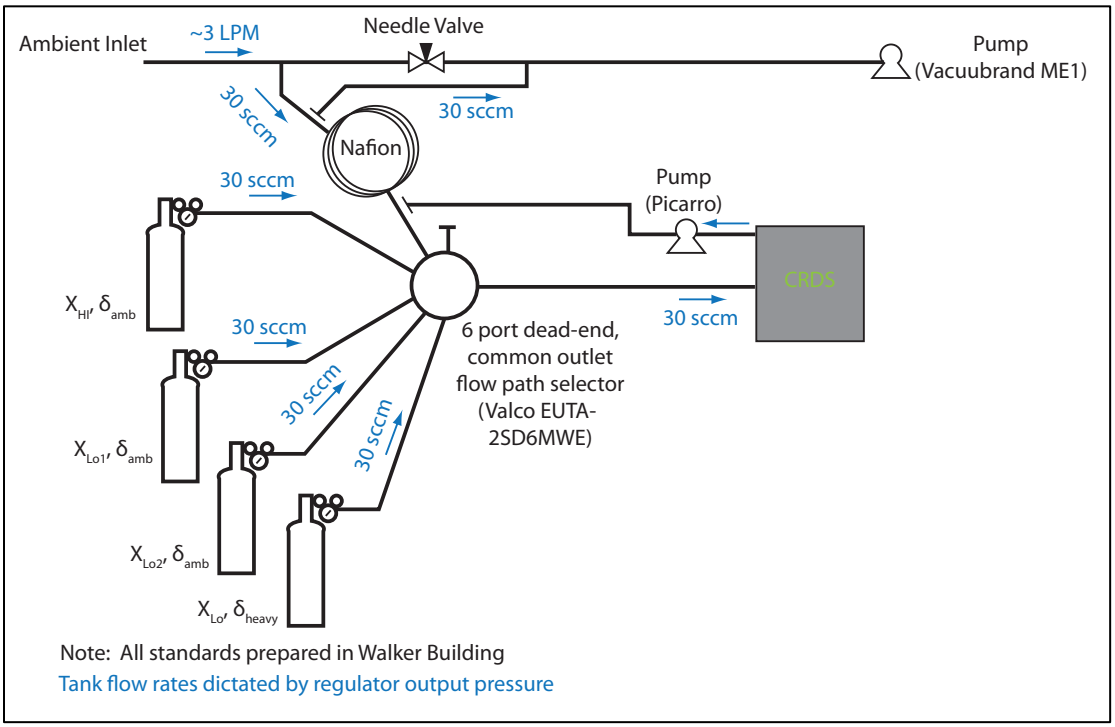

Figure 2: Field sampling flow schematic with automatic calibration system using four gas-phase standards of unique isotopic $^{13}CH_4$ values (δ) and CH_4 (X) mixing ratios at ambient (amb) and heavy and high (HI) and low (Lo1, Lo2) mixing ratios, respectively.

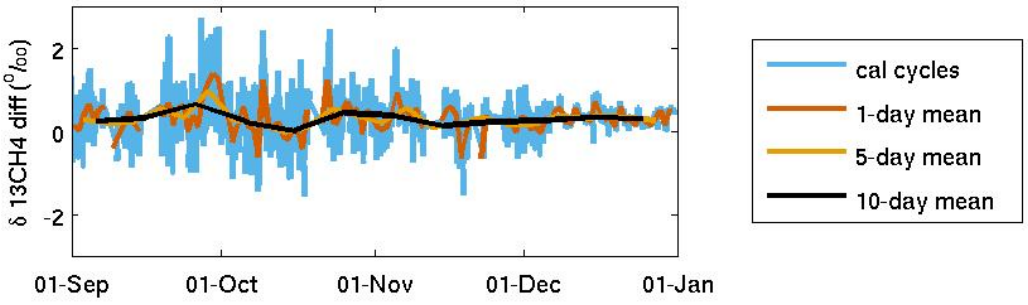

Figure 3. Low tank methane isotopic ratio differences from known value, for the individual calibration cycles, and for 1-, 5-, and 10-day means, for the South tower for September - December 2016. An improved calibration tank sampling strategy was implemented on 3 December 2016. The low tank is independent of the isotopic ratio calibration.

Throughout this project, four in-situ cavity ring-down spectrometers (G2132-i, Picarro, Inc.) measuring methane dry mole fraction (CH_4), carbon dioxide dry mole fraction (CO_2) and the isotopic ratio of methane ($\delta^{13}CH_4$) were deployed at four towers in the Marcellus Shale natural gas extraction region of Pennsylvania (Fig. 2). The data have been made available at the following URL: http://dx.doi.org/10.18113/D3SG6N.

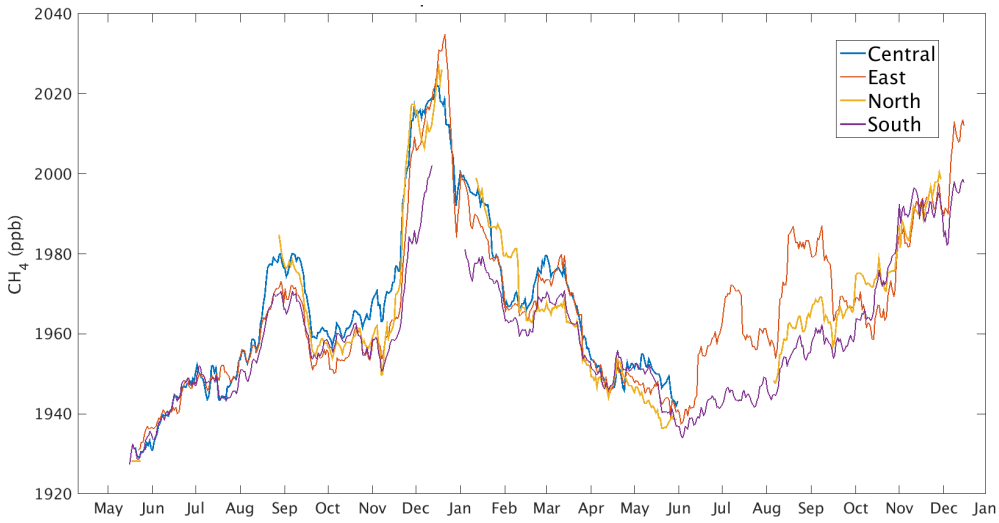

Figure 4**:** Atmospheric CH_4 mixing ratios in ppb collected at the four instrumented towers during the course of the project. Data are available at http://dx.doi.org/10.18113/D3SG6N.

The calibration of the continuous isotopic methane analyzers used in this study required both a linear calibration and a mole fraction correction, and a correction for cross-interference from ethane. We have submitted a paper (Miles et al., 2017, in review) to the journal *Atmospheric Measurement Techniques*. In the paper, we described laboratory and field calibration of the analyzers for tower-based applications, and characterize their performance in the field for the period January – December 2016. Prior to deployment, each analyzer was calibrated using high methane mole fraction air bottles with various isotopic ratios, from biogenic to thermogenic source values, diluted in zero air. Furthermore, at each tower location, three field calibration tanks were employed, from ambient to high mole fractions, with various isotopic ratios. By testing multiple calibration schemes, we determined an optimized field calibration method. A method to correct for cross interference from ethane is also described. Using an independent field tank for evaluation, the standard deviation of 4-hour means of the isotopic ratio of methane difference from the known value was found to be 0.26 ‰ $\delta^{13}CH_4$. Following improvements in the field calibration tank sampling scheme, the standard deviation of 4-hour means was 0.11 ‰, well within the target compatibility of 0.2 ‰. Round robin style testing using tanks with near ambient isotopic ratios indicated mean errors of –0.14 to 0.03 ‰ for each of the analyzers. Flask to in-situ comparisons showed mean differences over the year of 0.02 and 0.08 ‰, for the East and South towers, respectively.

Regional sources in this region were difficult to differentiate from strong perturbations in the background. During the afternoon hours, the median enhancements of isotopic ratio measured at three of the towers, compared to the background tower, were –0.15 to 0.12 ‰ with standard deviations of the 10-min isotopic ratio enhancements of 0.8 ‰ (Fig. 5). In terms of source attribution, analyzer compatibility of 0.2 ‰ $\delta^{13}CH_4$ affords the ability to distinguish a 50 ppb CH_4 peak from a biogenic source from one originating from a thermogenic source. Using a Keeling plot approach for the non-afternoon data at a tower in the center of the study region, we determined the source isotopic signature to be –31.2 ‰, consistent with a deep-layer Marcellus natural gas source (Fig. 6).

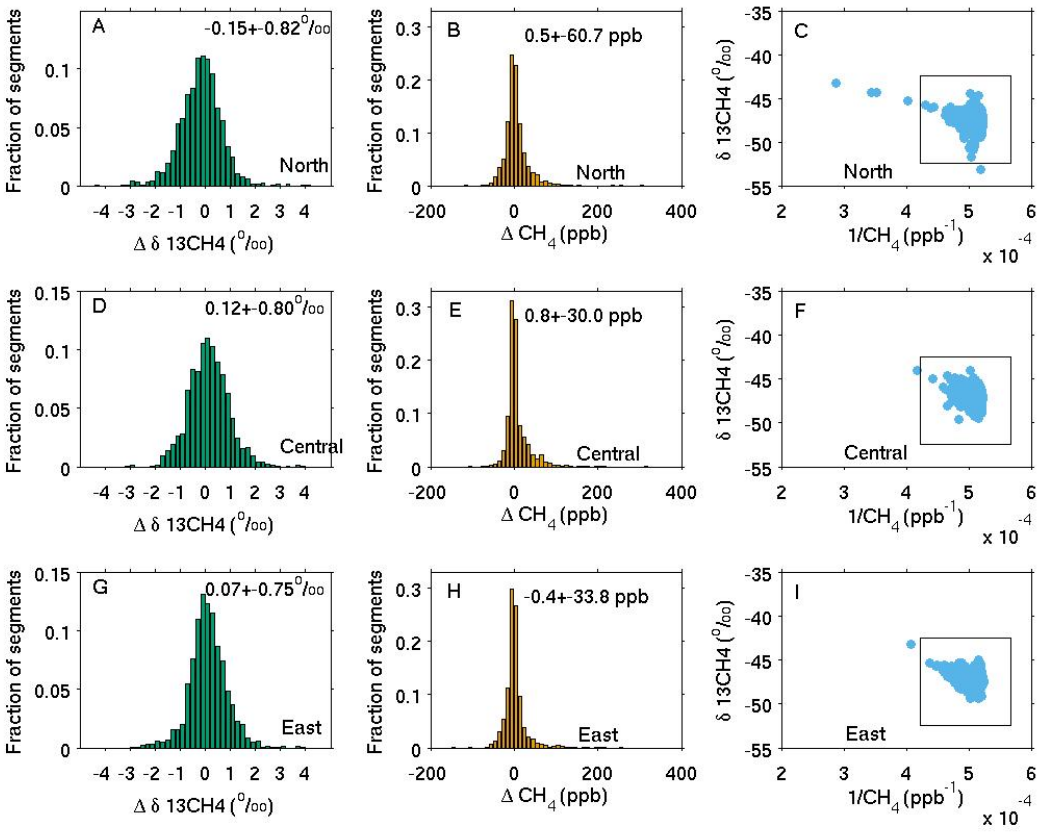

Figure 5: Probability distribution function of isotopic ratio enhancement above the background South tower for the A) North, D) Central, and G) East towers for afternoon hours (1700–2059 UTC, 1200–1559 LST). The time scale of the individual data points for all plots is 10 min and the time period is January – May 2016. The bin size for A), D) and G) is 0.2 ‰. Probability distribution function of methane mole fraction enhancements for the B) North, E) Central, and H) East towers. Note that the scale for B), E, and H) has been truncated to focus on majority of the data points. The bin size is 10 ppb CH_4. Keeling plots for the C) North, F) Central, and I) East towers. The black box in each plot indicates the approximate scale of the corresponding isotopic ratio enhancement and methane mole fraction enhancement plots.

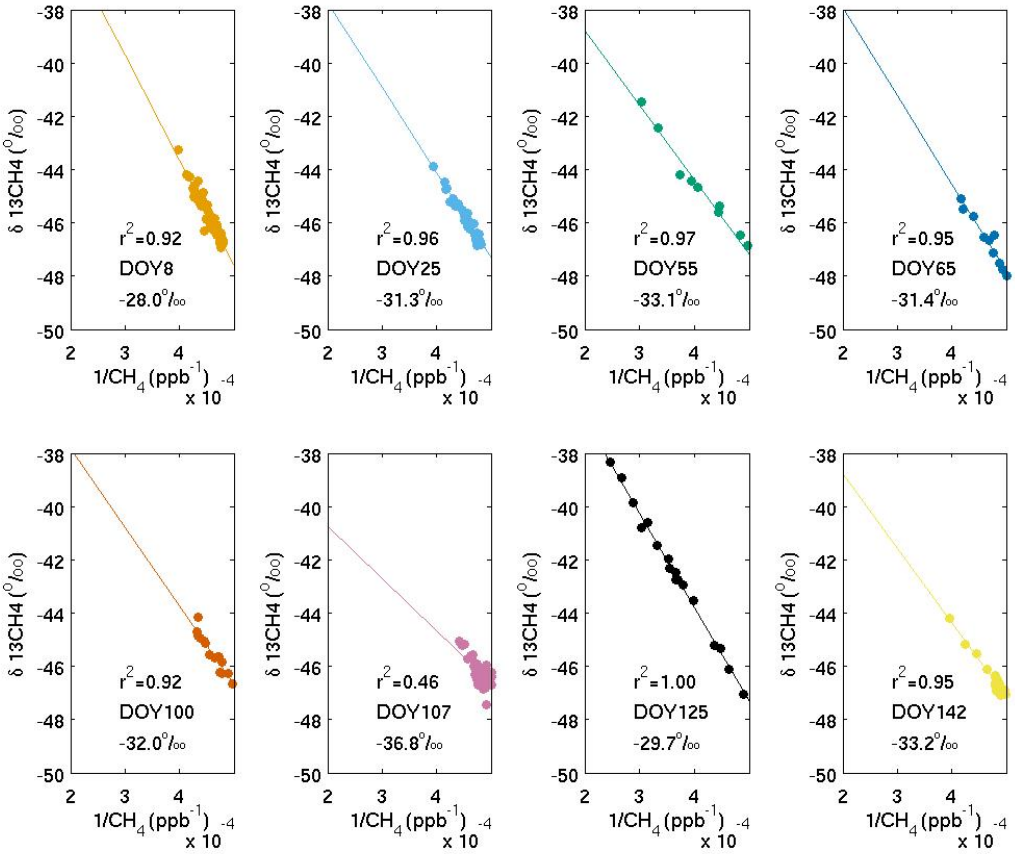

Figure 6: Keeling plots for the Central tower for the eight largest peak in the non-afternoon methane time series. Black lines indicate the best-fit lines. Correlation coefficients (r^2), day of year (DOY) and y-intercepts are indicated in the plots.

Subtask 3.2 Installation of the Portable Flask Packages for tracer sampling

Integrating flask sampling systems (Turnbull et al. 2012) were installed at the East and South towers in May, 2015 and the first samples were taken at the East tower in August and at the South tower in October, 2016. Flasks are filled over a 1-hour time period in the late afternoon (14-15 h local standard time), thereby yielding a more representative measurement, compared to most flask sampling systems, which collect nearly instantaneous samples (e.g. ~10 sec). The integrative sampling approach is particularly useful for flask samples taken nearby areas with large or variable surface flux processes (compared to those taken in remote regions). Back-trajectories from the HYSPLIT (Hybrid Single-Particle Lagrangian Integrated Trajectory, Stein et al. 2015) atmospheric transport and dispersion model are analyzed for each flask sample. Samples are measured only when winds were blowing steadily out of the west or north, to ensure that the samples were sensitive to and representative of the broader Marcellus shale gas production region that is the focus of this study.

For this project, more than 200 flask samples have been collected and measured for >55 gases (including greenhouse gases, hydrocarbons, and halocarbons) and $\delta^{13}CH_4$. The flask measurements are useful for independent validation and error-estimation of the continuous *in-situ* CO_2, CH_4, and $\delta^{13}CH_4$ measurements. Additionally, the many trace gases measured in the flasks provide information about the upwind source types.

The Flask Sampling Systems have been operated remotely during the entire period. The data set has been updated for recent flask samples (email request and access via http://cms.met.psu.edu/marcellus/site-data/).

Flask measurements were used for independent validation and error estimation of the continuous CO_2, CH_4 and $\delta^{13}CH_4$ in-situ measurements. In addition, the flasks were measured for a suite of species including N_2O, SF_6, CO, H_2 (Conway et al., 2011), halo- and hydro-carbons (Montzka et al., 1993) and stable isotopes of CH_4 (Vaughn et al., 2004). The flasks were filled over a 1-hour time period in the late afternoon (1400–1500 LST), thereby yielding a more representative measurement compared to most flask sampling systems, which collect nearly instantaneous samples (e.g., ~10 sec). Samples were measured only when winds were blowing steadily out of the west or north (~45–225°) to ensure that the samples are sensitive to and representative of the broader Marcellus shale gas production region that is the focus of this study.

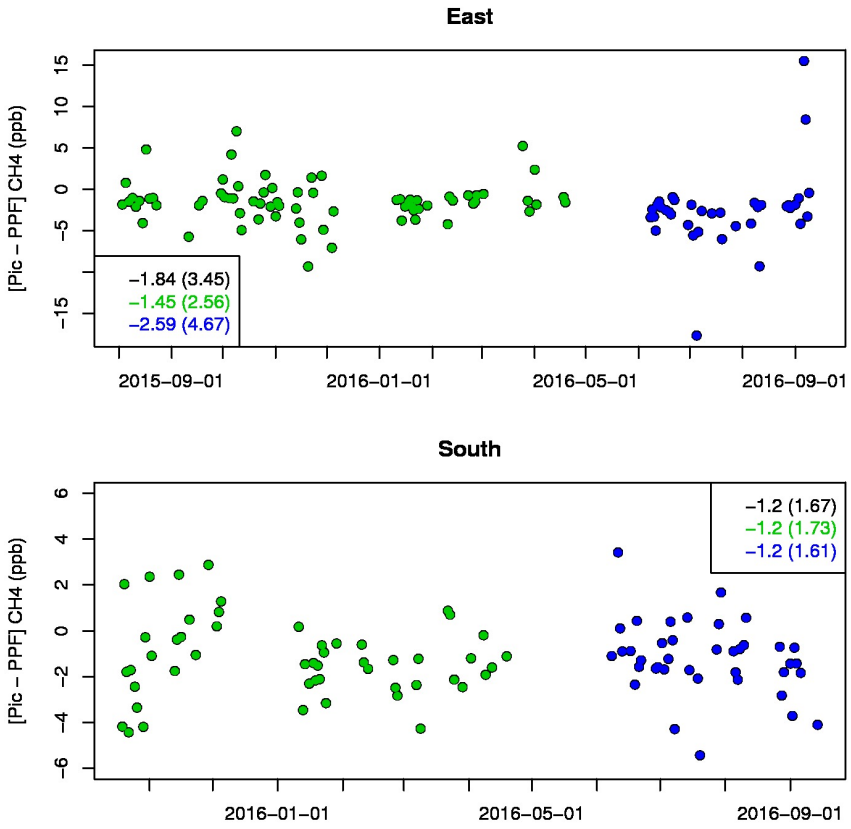

Figure 4: Hourly differences between continuous CH_4 mole fractions (CRDS Picarro) and flask samples at the East and South towers for the period August 2015 to September 2016

Further analysis of different trace gases measured in flasks provided a clear evidence that a large fraction of the elevated CH_4 mole fractions correspond to natural gas signals as indicated by synchroneous signals in hydrocarbon mole fractions. We show in Figure 5 the different tracer ratios by computing the slope of the linear regressions between different hydrocarbons. The residuals of the fit vary from 0.44 to 0.8 with a maximum between CH_4 and C_2H_6. For propane and other alkanes, lower correlation coefficients are observed which could be attributed to more variability in hydrocarbon contents (beyond ethane).

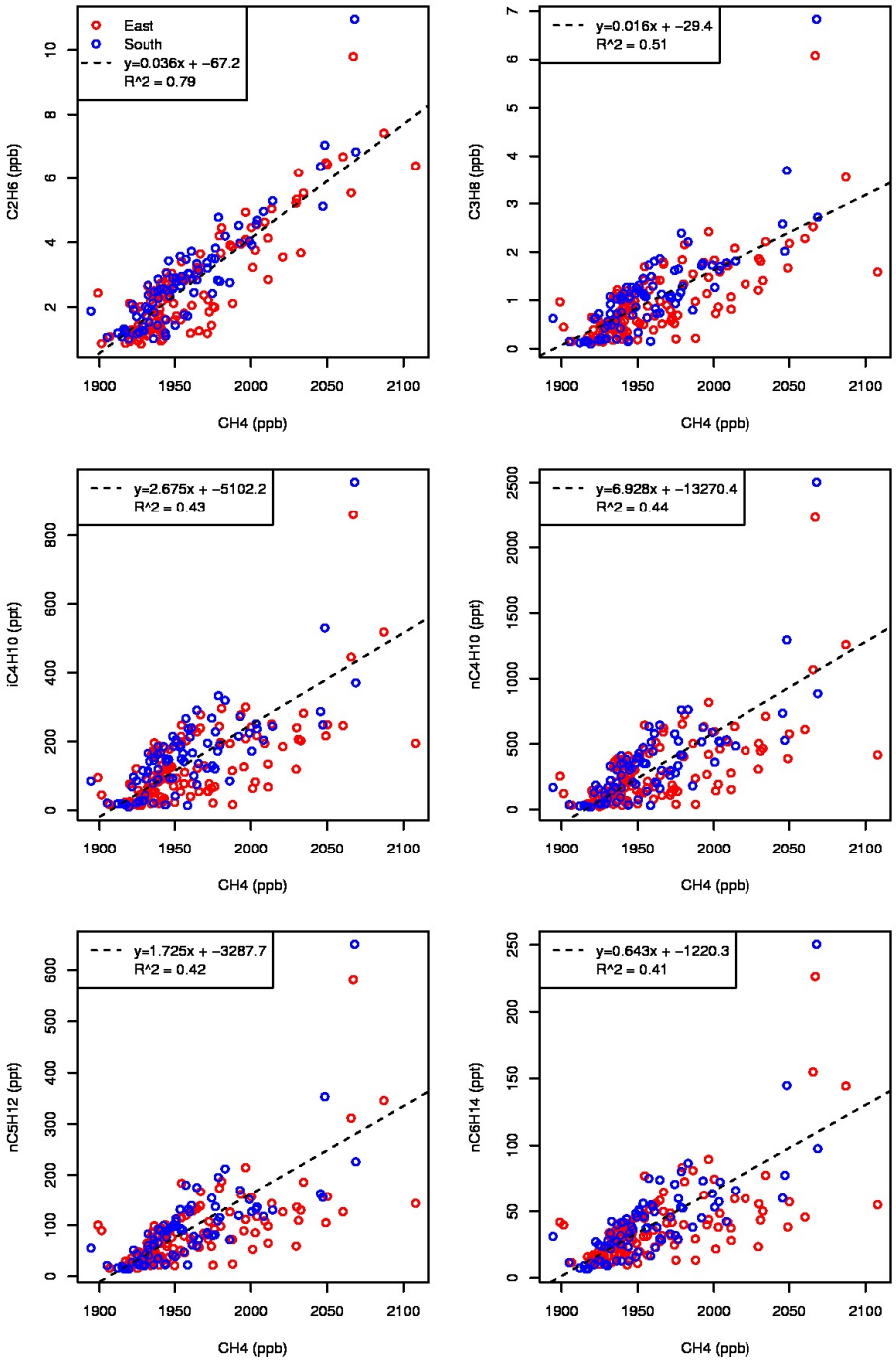

Figure 5: Tracer-to-tracer relationshps (slopes of linear regression) between CH_4 and other alkanes (longer chains) from flask samples collected at the East and South towers over the period August 2015 to September 2016.

Task 4 Regional CH_4 emission estimates using the surface network and mobile campaigns

Subtask 4.1 Aircraft campaign (May 2015)

An archive has been prepared and released for the public with a DOI (https://doi.org/10.15138/G35K54). The dataset is also discoverable on the NOAA ftp data finder (https://www.esrl.noaa.gov/gmd/dv/data/, site: MRC).

The results were published in Barkley et al. (2017) providing the first reliable estimate of emissions over the northeastern Marcellus shale. The leakage rate is equivalent to 0.4% of production (including wells and gathering compressors). Site-level estimate based on 15 sampled wells in PA (Omara et al., 2016) suggested a leakage rate of 0.64% of production (wells only). Wells in southwestern PA seems to produce large emission rates than in northeastern PA. EPA-derived estimate for NE PA (Maasakkers et al., 2016) suggest 0.13% of production for leakage rateAnd finally, a single aircraft mass-balance estimate by the NOAA Chemistry Monitoring Division over NE PA (Peischl et al., 2013) estimated 0.3% of production. These different studies seem to converge to lower emissions estimates than other shales across the US. The high production rates in the Marcellus shale seem to explain the relatively low CH_4 emissions across the state of PA. We will confirm these findings with a 2-year tower inversion but current findings suggest an emission rate of about 0.3 to 0.7% of production.

Continuous ethane (C_2H_6) measurements were collected during the aircraft campaign in 2015. Many thermogenic methane sources (oil and gas wells, coal mines) emit a small fraction of C_2H_6, whereas biogenic methane sources (wetlands, landfills, animal agriculture) do not have any C_2H_6 emissions. The amount of ethane emitted per methane molecule (i.e. ethane-to-methane or CH_4-to-C_2H_6 ratio) of thermogenic sources can vary. Oil wells and 'wet gas' wells contain higher ethane-to-methane ratios, while dry gas well and coal mines contain lower CH_4-to-C_2H_6 ratios. Thanks to the significant differences between these ratios, C_2H_6 measurements when plotted against CH_4 measurements can help with source attribution.

An Aerodyne C_2H_6 analyzer was instrumented in the Twin Otter during the campaing thanks to a collaboration with Dr. Eric Kort from the University of Michigan. The instrument specification and calibration are described in Kort et al. (2016) for the Bakken shale experiment. Based on the data collected from the Marcellus aircraft campaign, we intend to perform the first source attribution based on atmospheric measurements over the region. Observations of CH_4-to-C_2H_6 ratios calculated during 10 flights from the Spring 2015 campaign show a ratio of ~1.5% (Figure 8). A synthesis of individual tracer measurements from unconventional gas wells (Román-Colón and Ruppert, 2014) found that unconventional wells in our flight domain had an average CH_4-to-C_2H_6 ratio of 1.8%. The closeness of this number to our observed measurements from the campaign supports the hypothesis that most of the enhancements that were measured from this study were associated with the unconventional wells in the region. During the late flight on May 24th 2015, we see the largest CH_4-to-C_2H_6 ratios observed during the campaign. On this day, we suspect enhancements from coal and gas sources from southwest Pennsylvania based on model simulations performed previously (Barkley et al., 2017). The plumes from SW PA were intruding into our flight area. The wells from the southwestern portion of the state contain "wet gas", and have higher CH_4-to-C_2H_6 ratios (up to 7%) compared to the gas in northeastern Pennsylvania. This likely explains the higher ratios observed during this flight. Similarly, on May 29th, the CH4 enhancements originated from sources in Virginia and West Virginia, which also includes mining activities and higher CH_4-to-C_2H_6 ratios.

From this study, we estimate an emission rate between 0.27% and 0.45% of gas production using the model optimization method and 0.08–0.72% of gas production using the aircraft mass balance with a 2σ confidence

interval. Figure 7 provides the emission range estimates from upstream natural gas processes using both the model optimization technique and mass balance technique when applicable. Top-down studies of other basins in the USA have all found emission rates greater than 1% of production, and thus the rates calculated for the north-eastern Marcellus basin are the lowest observed yet, raising questions as to why the values in this region ap- pear to be low. One possibility may be related to the high efficiency of the north-eastern Marcellus region compared to other major shale plays. In terms of gas production per unconventional well, the Marcellus is the highest of all major basins in the USA. Furthermore, the gas production per well increases by nearly a factor of two when focusing specifically on Susquehanna and Bradford counties in north- eastern Pennsylvania where the majority of the wells from this study are located. The large difference in production per well between the north-eastern Marcellus and other shales may partly explain the low emission rates as a percentage of production. Throughout this study, we normalize natural gas emissions as a percentage of total production under the assumption that higher throughput of natural gas in a system should lead to higher emissions in the system. However, if leaks are more influenced by the number of components in operation rather than by the throughput passing through the wells, a high production-per-well system such as the uncon- ventional wells in the north-eastern Marcellus could end up having a very low emission rate as a percentage of production but a similar emission rate compared to other basins based on the number of wells, compressors, etc. A thorough bottom-up study of the Marcellus region measuring emissions on a device level could provide an answer to this hypothesis.

Although we calculate a low emission rate for this region, rates calculated for 22 and 25 May stand out as outliers where emissions fall well above our uncertainty bounds. It is possible that emissions from natural gas sources were higher on these days compared to others. Releases of natural gas into the atmosphere from short time frame events, such as liquids unloading and venting, can add a temporal component to the emission rate. Such events occurring at an increased frequency during the 22 and 25 May flights could be responsible for the higher emission rates. However, these 2 days have issues that could have affected the optimized emission rate. On 22 May, we observe a sudden drop in the observed CH_4 values that is nearly as large as the main plume on that day, creating concerns about background concentrations. On 25 May, a south-westerly wind was present, and while the model showed the coal plume to be west of the flight path, a small shift in the model wind direction would shift the coal plume over the region. For these reasons we are sceptical but not dismissive of the high emission rates found during these two flights.

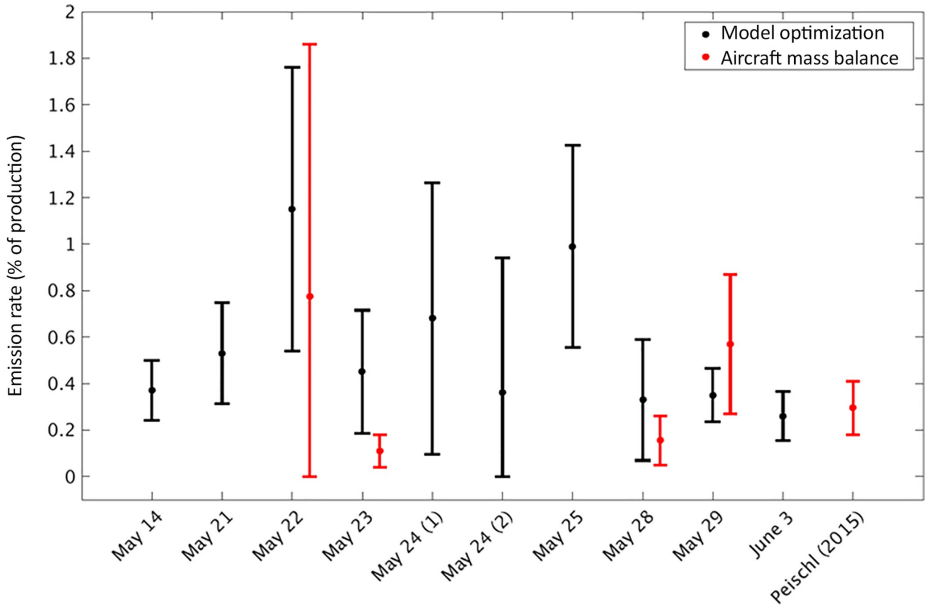

Figure 7: Calculated upstream natural gas emission rates using (black) model optimization technique and (red) aircraft mass balance technique. Error bars represent the 2σ confidence interval for each flight. Mass balance performed in Peischl et al. (2015) included for comparison.

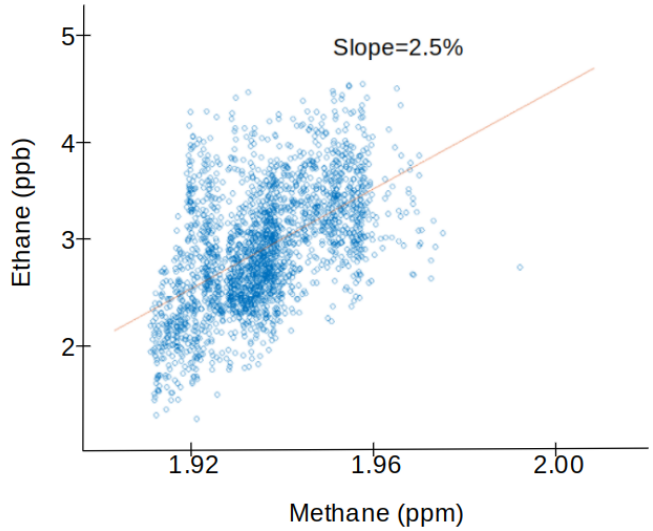

Figure 8: Measured CH_4 vs. C_2H_6 observations from the late-afternoon flight on May 24th, 2015 corresponding to elevated CH_4-to-C_2H_6 ratios from SW PA. Coal mines and wet gas wells present larger values than dry gas from NE PA, therefore confirming the presence of other sources due to long distance transport.

Subtask 4 .2 Automobile measurements of isotopic signature to identify CH_4 sources

Methane (CH_4) measurements were conducted using a cavity ring-down spectrometer (Model G2301-f, Picarro, Inc.) onboard a mobile, on-road platform. Approximately 3,267 km and 57 hours were collected throughout the northeast PA Marcellus Shale region. The measurements were collected between 12 May - 4 June, 2015. The median of the CH_4 dry mole fractions over the entire campaign was 1.90 ppmv and the 5th and 95th percentiles were 1.87 and 2.05 ppmv, respectively. Elevated CH_4 (i.e. above the 95th percentile), have been preliminarily attributed to cattle farms, landfills, regional coalmines and natural gas drilling activities. The second automobile campaign confirmed the absence of large unreported sources in the region. The detected enhancements along the drive corresponded systematically to a known emitter in the area. The largest emitters were usually the compressor stations, in agreement with inventory estimates and other field studies. Multiple CH_4 plumes were measured near dairy farms but the overall contribution remains small, as expected from reported emissions. A data mining analysis was performed in collaboration with Prof. Jessie Li, from the College of Information Sciences and Technology of Pennsylvania State University to indetify outliers in the drive-around measurements of CH_4 and $^{13}CH_4$. The method has been published at the 23rd ACM SIGKDD International Conference on Knowledge Discovery and Data Mining (Zheng et al., 2017).

Subtask 4.3 Inverse estimates of CH_4 emissions from the surface tower network

Initially, all emissions calculations using our Lagrangian Particle Dispersion Model (LPDM) were performed on pseudo-data to better understand the capabilities and limitations of our inverse modelling network. The results showed that given perfect transport, our tower network should be able to detect the presence of any large point sources of methane in the region and the posterior flux field calculated using the inversion would be able to successfully locate them spatially. With this determined using pseudo-data, we then moved to using the true tower observations to see if these conclusions would hold. For this experiment, hourly methane observations between 17-21Z were averaged for the day and used from all four towers between the periods of September 2015 through December 2015. The background tower was selected based on wind direction provided by the model during the afternoon hours, and its footprint was subtracted off of the footprints of the downwind towers. Days with an average wind speed of less than 3 m/s were removed to ensure that the air measured at the background tower had time to move to the downwind towers during the afternoon. The months selected for this experiment was due to a lack of available model data for tower measurements in 2016. Future work will use all available tower observations from 2015 and 2016 when model data becomes available.

Initial results from this experiment were not robust. With more than 500 gridpoints in our 3km resolution gridded inventory containing at least one unconventional well in addition to the large variability of emissions a well would have, the solutions for the posterior flux were under-constrained; small changes to the observations used or the uncertainty parameters set in the inversion would result in a different spatial distribution of the natural gas emissions, though the total emissions from natural gas production were always lower than the prior estimate. To better constrain the problem, the gridded inventory was grouped into 29 different sectors (Figure 9). By reducing the number of points to solve for by creating these unique sectors, the inversion loses the ability to identify individual super-emitters, but instead is able to quantify the emission rate over these different sub-regions, allowing us to find areas where emissions may be higher or lower than expected. Figure 10 shows the change between the prior and posterior emissions inventory for these different sectors using the tower data from October 2015 to December 2015.

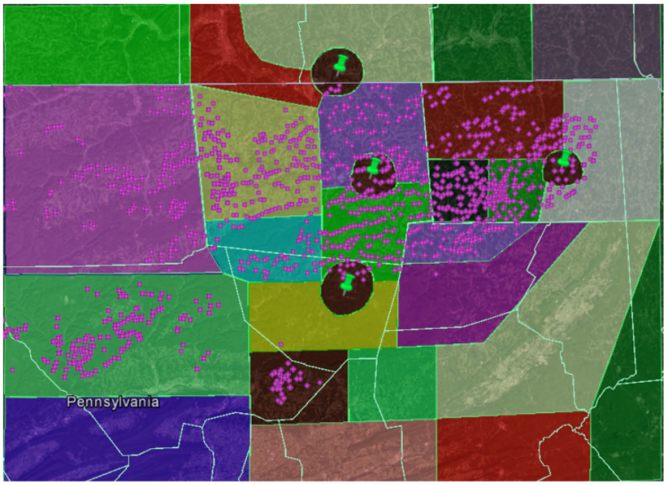

Figure 9: Diagram of the different flux sub-regions used in the inversion. Towers (green pins) and wells (pink dots) are plotted overtop

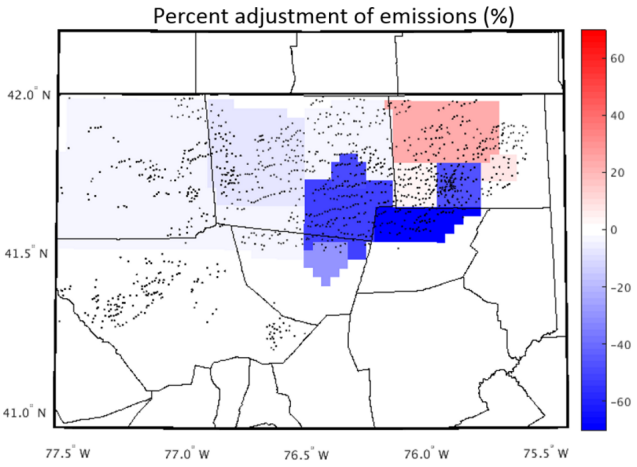

Figure 10: Map of the percent change in the posterior flux compared to the prior flux using tower observations from Oct-Dec 2015.

To define the optimal tower locations, we used a Langragian Particle Dispersion model (LPDM) to map out an "influence function" for a given tower. Using LPDM, we can trace the path of air parcels at our tower location backwards in time and find the areas within our model domain that contribute to the CH_4 concentrations observed at that tower. Influence functions have been produced for each of the 4 towers for all hours between September 2015 to October 2016. A subset of the data is presented in Figure 11. We explore the best background mixing ratios on average at the different towers in Figure 12. The accumulation of low and high values inform us about the regional and far-field signals observed at the four towers. The South tower is the most representative of the regional background when the wind is from the South and the West. For northerly winds, the North tower is the best background, which is consistent with the relative location of the site. We conclude here that the South tower is likely to be selected as our background in most wind conditions, except under northerly flow.

Using these modeled influence functions in conjunction with observational tower data, we can perform an experiment to find hotspot locations for potential emitters. Figure 13 shows an example of how this is done for East tower. From the observational data, we pick out all of the hours where a given tower records the highest CH_4 mole fraction among all of the towers. We then take the influence functions from these hours and average them, giving us a mean influence function which is most common for a given tower when that tower has the largest enhancement. We then repeat this averaging process, but this time using influence functions for hours where that tower has the smallest observed CH_4 mole fraction, giving us a mean influence function for a tower during periods when its enhancement is smallest. We can then subtract these two different influence function maps and create a map which reveals what areas of influence commonly result in higher and lower enhancements for a given tower site. For example, in Figure 13, we can see that the influence functions for East tower which occur on days where East tower records the highest observation of the four towers are often west of the tower site. This intuitively makes sense, as the majority of the unconventional wells are west of the tower, and so one would expect a westerly wind to produce higher observed concentrations at the site.

On their own, these mean influence functions produced for each tower do not provide much information about emission hotspots. But if you average together the mean influence function across all four towers, the hotspots which are common among all site locations become more apparent and provide information on where major methane sources might that impact the region.

Upon inspecting Figure 13, many interesting hotspots appear that correlate with our expectations from the methane inventory created for this project. Immediately we see the hotspot which has the strongest correlations with high methane observations is the region of unconventional wells, illustrating the dominance that emissions from upstream gas sources have on our tower readings. But multiple smaller hotspots can be seen at areas with large amounts of natural gas distribution, including cities such as New York, Philadelphia, and Buffalo. In addition to natural gas sources, we see a stripe of high influence appear in southwestern PA where both unconventional wells and large coal beds reside. In addition to areas where the hotspots match our expectations, there are a few curious patterns where areas of high influence appear where we would not otherwise have expected it. A north-south stripe passing through the Finger lakes and another stripe that passes through Williamsport are both regions where we do not have large methane emitters recorded in our inventory. As more data comes in from the towers and more footprints are created, these hotspots should become more refined, and provide more confidence on the location of large methane emitters in the region.

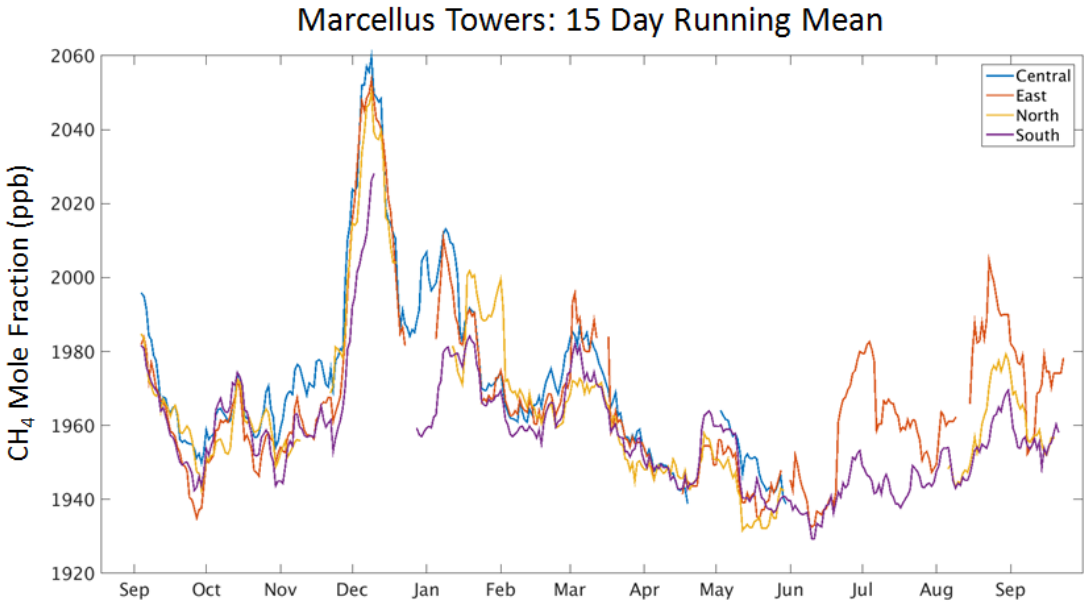

Figure 11: Observed CH_4 mole fractions at each of the four tower locations from September 2015 to September 2016.

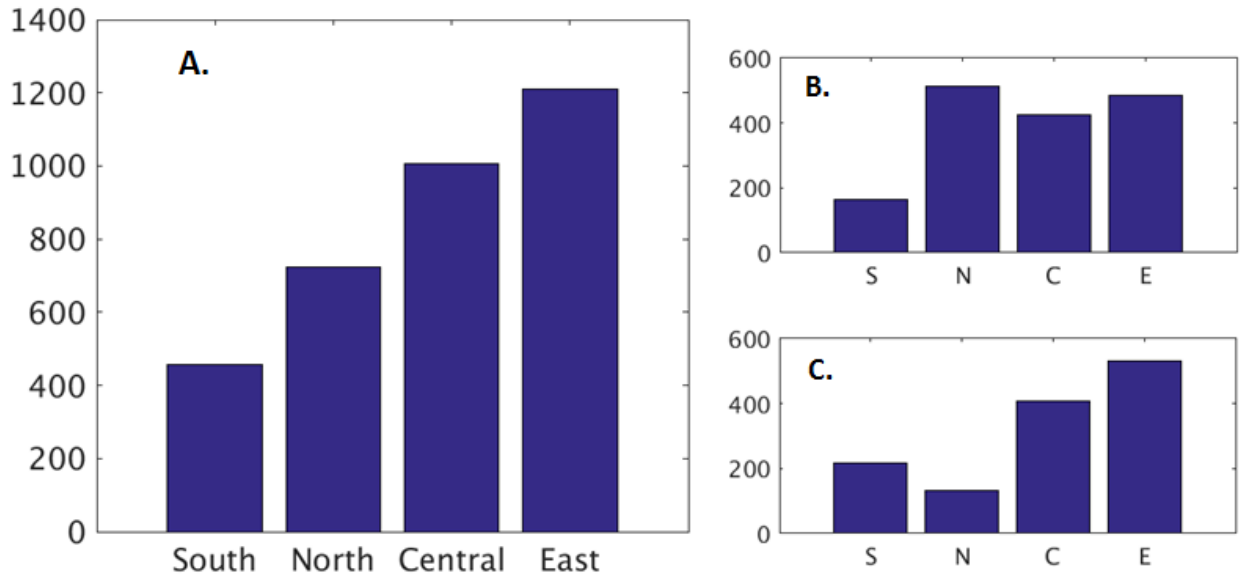

Figure 12: a.) Number of hourly intervals in which each tower recorded the largest CH_4 mole fraction compared to all other towers. b.) Same as a. but using only hourly periods where the mean wind direction had a southerly component. c.) Same as a. but using only hourly periods where the mean wind direction had a northerly component.

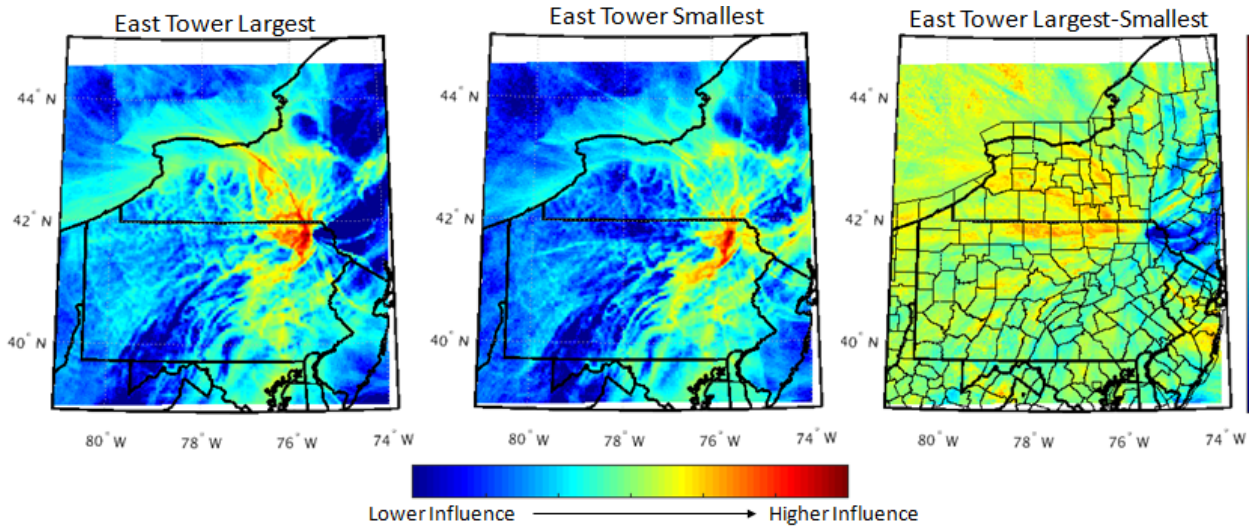

Figure 13: Average influence functions calculated at East tower for hours when East tower recorded the (left) highest CH_4 observation, and (center) lowest CH_4 observation among all four towers. (right) A map showing the subtraction of the center figure from the left figure. Warmer colors in this figure illustrate footprints which correspond with periods when East tower observes its highest CH_4 concentrations, whereas cooler coolers are common footprints on periods where East tower records its lowest CH_4 concentrations compared to other towers.

Subtask 4.4 Comparison of inverse modeling estimate to regional aircraft and automobile results - Evaluation of the uncertainties

Based on the results from 4.1 and 4.3, we evaluated the uncertainty assessment as detailed in Barkley et al. (2017). From the WRF modeling system optimization, we estimate an emission rate between 0.27% and 0.45% of gas production, and 0.08–0.72% of gas production using the aircraft mass balance with a 2σ confidence interval. For both methods, the mean is around 0.4% of production. Based on the Bayesian inversion of the tower data for October to December 2015, we found a slight decrease in emissions from the 0.13% emission rate used in the prior. Overall, the tower inversion suggests even lower emissions over the period, with only the wells along the Pennsylvania northern tier counties showing any increase. These results, compared to the results from the Marcellus aircraft campaign, indicate lower emissions for the period October to December 2015. However, later time periods vary significantly as suggested by the large variations in the observed atmospheric CH_4 enhancements (cf. Figure 14). Therefore, we expect significant increase for periods of 4-6 weeks during the 18 months of the tower deployment. As a conclusion, the low emission rate from the tower inversion matches the lower-bound estimate of the mass-balance approach using the aircraft data.

Task 5 Life-cycle assessment of CH_4 emission estimates over the 2 years of deployment and reporting of emission factors for the northern Marcellus region

Subtask 5 .1 Temporal development of gas activities and inverse CH_4 emission estimate

Druing the 18 months of deployment, we observed both large scale variations that enhanced the CH_4 mixing ratios of the four instrumented towers, and signal variations observed by a subset of the four towers, due to variations in local CH_4 emissions. To extract these local emission signals, we need to subtract the overall background (large-scale variations) from all the towers at any given time. The residuals correspond to local-scale variations. When considering the mixing ratios presented in Figure 13, several time periods present higher tower-to-tower differences, which suggest that local emissions increased significantly. The background mixing ratios were quantified using the upwind tower for each day, based on wind measurements. We then calculated the differences between the background tower (changing each day) and the other towers. We plotted these differences in Figure 14 as a function of time, highlighting the enhancements due to local sources (i.e. NE PA). The tower-to-tower differences reach 25ppm on average from December 2015 to February 2016 and from June to the end of September 2016. This increase is signifcant compared to our initial inversion time period (from October to December 2015) with an average of 5ppm over the period, which assumes that emissions were multiplied by 2-5 times during several months. The origin of the enhancements could be due to natural gas activities but also to other methane emitters in the area. The WRF mesoscale simulations in Four-Dimensional Data assimilation (FDDA) mode has been performed, and tower footprints have been calculated using the LPDM at 1km resolution. A complete regional inversion assessment will be published in the coming months.

Figure 14**:** Atmospheric CH_4 mixing ratio enhancements (in ppm) measured across the tower network from May 2015 to January 2017.

Subtask 5 .2 Life-cycle CH_4 emissions using the inverse estimates and gas activity data

We have contacted gas companies and got access to drilling information to analyze our weekly CH_4 emissions estimates over the 29 regions defined for NE PA. Of primary interest is the production data from wells, but also reported failures in the region. Our analysis suggests large unreported emissions over 4- to 6-weekly time periods which could increase the overall emissions from the region. However, the increased periods of the inverse emissions remains diffcult to relate to a specific event, as some of the activities are not publicly accessible. The absence of gas processing units and the small emissions from pipelines (as reported from other studies) suggest that these high emissions originate from the production sector. A more detailed analysis of the gas company activities would be needed to identify the possible events related to the observed peaks. In the future, access to activity data would help attribute the high emission rates observed during the deployment.

Products developed under the award and technology transfer activities

Conferences

Barkley, Lauvaux, Davis, Murphy, Miles, Richardson, Sweeney, McKain. Long-term atmospheric monitoring of CH4 emissions from Gas Production activities in the Marcellus shale area. U.S. Environmental Protection Agency 2017 International Emissions Inventory Conference, Baltimore, August 2017.

Miles, Martins, Richardson, Rella, Lauvaux, Davis, Barkley, McKain, and Sweeney. Calibration and Field Testing of Cavity Ring-Down Laser Spectrometers Measuring CH4 Mole Fraction and the Isotopic Ratio of 13CH4 and Deployed on Towers in the Marcellus Shale Region. Poster presented at the NOAA GMD Annual Meeting, Boulder, CO, May 2017.

Li Z, Zheng G, Agarwal A, Xue L, and Lauvaux T: Proceedings of the 2017 SIAM International Conference on Data Mining. 2017, 804-812 , 2017.

Miles, Martins, Richardson, Rella, Lauvaux, Davis, Barkley, McKain, Sweeney. Calibration and Field Testing of Cavity Ring-Down Laser Spectrometers Measuring Methane Mole Fraction and the Isotopic Ratio of Methane Deployed on Towers in the Marcellus Shale Region. Poster presented at the Joint NACP and Ameriflux Prinicipal Investigators Meeting, North Bethesda, MD, March 2017.

Cao, Cervone, Barkley, Lauvaux, Deng, Miles, Richardson. Characterization of Methane Emission Sources Using Genetic Algorithms and Atmospheric Transport Modeling. Poster A51K-0224, 2016 Fall AGU Meeting, San Francisco, CA, December 2016.

Barkley, Lauvaux, Davis, Deng, Miles, Richardson, Martins, Cao, Sweeney, McKain, Schwietzke, Smith, Kort. Top-down Estimate of Methane Emissions from Natural Gas Production in Northeastern Pennsylvania Using Aircraft and Tower Observations. Presentation A54G-03, 2016 Fall AGU Meeting, San Francisco, CA, December 2016.

Barkley, Davis, Lauvaux, Deng, Martins, Miles, Richardson, Cao, Karion, Sweeney, Schwietzke, McKain, M. Smith and Kort. Methane emissions from natural gas production in Pennsylvania: Aircraft model comparison. Talk presented at the NOAA GMD Annual Meeting, Boulder, CO, May 2016.

Miles, Richardson, Martins, Rella, Lauvaux, Davis, Barkley, McKain, Sweeney, Karion. Tower-Based measurements of CH4 dry mole fraction and delta 13CH4 in the northeastern Pennsylvania Marcellus Shale Gas Region. Poster presented at the NOAA GMD Annual Meeting, Boulder, CO, May 2016.
Available at: http://sites.psu.edu/marcellus/wp-content/uploads/sites/4208/2014/02/Miles_NOAA_GMD_Poster_Final-1.pdf

Lauvaux T., Z. Barkley, K.J. Davis, N. Miles, S. Richardson, D. Martins, Y. Cao, E. -K. Kim, G. Cervone, A. Taylor, C. Sweeney, A. Karion, K. McKain, T. Murphy: Regional methane emissions estimates in northern Pennsylvania gas fields using atmospheric inversions, RPSEA ONSHORE TECHNOLOGY WORKSHOP: Emissions from Unconventional Resources Development Activity, May 26, 2016 Denver Athletic Club

Barkley Z., K. Davis, T. Lauvaux, N. Miles, S. Richardson, D. Martins, A. Deng, Y. Cao, C. Sweeney, A. Karion, M. Smith, E. Kort, S. Schwietzke: Constraining Methane Emissions from Natural Gas Production in Northeastern Pennsylvania Using Aircraft Observations and Mesoscale Modeling, AGU 2015 Fall meeting, A11J-0199, San Francisco, CA, 2015.

Lauvaux T., Z. Barkley, D. Martins, S. Richardson, K.J. Davis, N. Miles: "Continuous, Regional Methane Emissions Estimates in Northern Pennsylvania Gas Fields Using Atmospheric Inversions", Department of Environmental Protection, 23 November 2015, Harrisburg, PA.

T. Lauvaux, "Continuous, Regional Methane Emissions Estimates in Northern Pennsylvania Gas Fields Using Atmospheric Inversions", Shale Alliance for Energy Research (SAFER) Technical Briefing, State College, August 20, 2015. Avail. online at http://www.saferpa.org/Pages/Technical-Briefing-08-2015.aspx

Martins, Lauvaux, Miles, Richardson, Barkley, Deng, Gaudet, Davis, Cao, Taylor, 2015: Continuous, regional methane emissions estimates in northern Pennsylvania gas fields using atmospheric inversions. Poster presented at the 5th North American Carbon Program Principal Investigators Meeting, Washington, D,C., January 2015.

Lauvaux, Deng, Gaudet, Richardson, Miles, Ciccarelli, and Davis: Regional methane emissions estimates in northern Pennsylvania gas fields using a mesoscale atmospheric inversion system, presented at the 94th Annual Meeting of the American Meteorological Society, Atlanta, GA; 2-6 February 2014.
Available at: http://sites.psu.edu/marcellus/publications/

Peer-reviewed articles

(In Preparation)

Barkley, Z. R., Lauvaux, T., Davis, K. J., Dickerson, R., Ren, X., Deng, A., et al.: Emissions of CH4 from Unconventional shale gas and coal mines in the southwestern Marcellus Shale.

Barkley, Z.R., Lauvaux, T., Davis, K.J., Deng, A., Sweeney, C., Martins, D., Miles, N.L., Richardson, S. J., Murphy, T., Karion, A., Maasakkers, J. D.: Long-term monitoring of regional methane emissions from natural gas production in northeastern Pennsylvania.
Submitted:

Miles, N. L., Martins, D. K., Richardson, S. J., Rella, C. W., Arata, C., Lauvaux, T., Davis, K. J., Barkley, Z. R., McKain, K., and Sweeney, C.: Calibration and Field Testing of Cavity Ring-Down Laser Spectrometers Measuring CH4, CO2, and δ13CH4 Deployed on Towers in the Marcellus Shale Region, Atmos. Meas. Tech. Discuss., https://doi.org/10.5194/amt-2017-364, in review, 2017.

(Published)

Barkley, Z. R., Lauvaux, T., Davis, K. J., Deng, A., Miles, N. L., Richardson, S. J., Cao, Y., Sweeney, C., Karion, A., Smith, M., Kort, E. A., Schwietzke, S., Murphy, T., Cervone, G., Martins, D., and Maasakkers, J. D.: Quantifying methane emissions from natural gas production in north-eastern Pennsylvania, Atmos. Chem. Phys., 17, 13941-13966, https://doi.org/10.5194/acp-17-13941-2017, 2017.

Cao, Y., Cervone, G., Barkley, Z., Lauvaux, T., Deng, A., and Taylor, A.: Analysis of errors introduced by geographic coordinate systems on weather numeric prediction modeling, Geosci. Model Dev., 10, 3425-3440, https://doi.org/10.5194/gmd-10-3425-2017, 2017.

Zheng, G., Brantley, S. L., Lauvaux, T., Li, Z. Contextual Spatial Outlier Detection with Metric Learning. Proceedings of the 23rd ACM SIGKDD International Conference on Knowledge Discovery and Data Mining (KDD '17), 2161-2170, doi:10.1145/3097983.3098143, 2017.

Project website

The results of the project and the information related to the deployment are available at:
http://sites.psu.edu/marcellus/

Data sets publicly available

Automobile Megacore mixing ratios
Megacore data have been collected for multiple drive-around campaigns in northeastern PA. The first data set is available at: http://sites.psu.edu/marcellus/data-download/mega-core-data/
Other data can be accessed by emailed request to: CO2DATA@meteo.psu.edu

Continuous atmospheric mixing ratios
Throughout this project, four in-situ cavity ring-down spectrometers (G2132-i, Picarro, Inc.) measuring methane dry mole fraction (CH_4), carbon dioxide dry mole fraction (CO_2) and the isotopic ratio of methane ($\delta^{13}CH_4$) were deployed at four towers in the Marcellus Shale natural gas extraction region of Pennsylvania. The data have been made available at the following URL: http://dx.doi.org/10.18113/D3SG6N

Miles, N.L., D.K. Martins, S.J. Richardson, T. Lauvaux, K.J. Davis, B.J. Haupt, and C. Rella, 2017. In-situ tower atmospheric methane mole fraction and isotopic ratio of methane data, Marcellus Shale Gas Region, Pennsylvania, USA, 2015-2016. Data set. Available on-line [http://datacommons.psu.edu] from The Pennsylvania State University Data Commons, University Park, Pennsylvania, USA. http://dx.doi.org/10.18113/D3SG6N.

Discrete trace gas samples (Automated Flask Samplers)
The Automated Flask Samplers have been operated during the entire project, collecting air samples over 2 years. The 55 trace gases analyzed in each flask are available at:
ftp://aftp.cmdl.noaa.gov/data/campaign/Marcellus_2015/

Aircraft atmospheric mixing ratios
These data were collected aboard a NOAA Twin Otter aircraft based in # Williamsport, Pennsylvania in May and June of 2015. Research flights covered the Marcellus Shale region in northeastern Pennsylvania. This dataset is comprised of continuous measurements of CH_4, CO_2, $^{13}CH_4$, H_2O mole fractions from a Picarro cavity ring-down spectrometer operated by the NOAA ESRL group, and C_2H_6 mole fractions from an Aerodyne laser absorption spectrometer operated by the University of Michigan group. Other parameters reported in this dataset are GPS location, course over ground, ground elevation, wind speed and direction, and ambient temperature, pressure and relative humidity. All measurements are given to the nearest 1-second. An archive has been prepared and released for the public with a DOI (https://doi.org/10.15138/G35K54). The dataset is also discoverable on the NOAA ftp data finder (https://www.esrl.noaa.gov/gmd/dv/data/, site: MRC).

Sweeney, C., A. Karion, E.A. Kort, M.L. Smith, T. Newberger, S. Schwietzke, S. Wolter, T. Lauvaux (2015), Aircraft Campaign Data over the Northeastern Marcellus Shale, May-June 2015, Version: 2017-03-29, Path: https://doi.org/10.15138/G35K54.

Modeling system (Atmospheric model)

The atmospheric transport model used in this study is the Advanced Weather Research and Forecasting (WRF) model (WRF-ARW, Skamarock et al., 2005) version 3.6.1. The WRF configuration for the model physics used in this re- search includes the use of (1) the double-moment scheme (Thompson et al., 2008) for cloud microphysical processes, (2) the Kain–Fritsch scheme (Kain and Fritsch, 1990; Kain, 2004) for cumulus parameterization on the 9 km grid, (3) the rapid radiative transfer method for general circulation models (GCMs) (RRTMG, Mlawer et al., 1997; Iacono et al., 2008), (4) the level 2.5 TKE-predicting MYNN planetary boundary

layer (PBL) scheme (Nakanishi and Niino, 2006), and (5) the Noah 4-layer land-surface model (LSM), which predicts soil temperature and moisture (Chen and Dudhia, 2001; Tewari et al., 2004) in addition to sensible and latent heat fluxes be- tween the land surface and atmosphere.

The WRF model grid configuration used in this research contains two grids, 9 and 3 km, each with a mesh of 202x202 grid points. The 9 km grid contains the mid-Atlantic region, the entire north-eastern United States east of Indiana, parts of Canada, and a large area of the northern Atlantic Ocean. The 3 km grid contains the entire state of Pennsylvania and most of the state of New York. Fifty vertical terrain-following model layers are used, with the centre point of the lowest model layer located at 10 m above ground level. The thickness of the layers stays nearly constant with height within the lowest 1 km, with 26 model layers below 850 hPa (1550 m a.g.l.). One-way nesting is used so that information from the coarse domain translates to the fine do- main but no information from the fine domain translates to the coarse domain.

The WRF modelling system used for this study also has four-dimensional data assimilation (FDDA) capabilities to allow meteorological observations to be assimilated into the model (Deng et al., 2009). With WRF FDDA, observations are assimilated through the entire simulation to ensure the optimal model solutions that combine both the observation and the dynamic solution, a technique referred to as dynamic analysis. Data assimilation can be accomplished by nudging the model solutions toward gridded analyses based on observations (analysis nudging) or directly toward the individual observations (observation nudging), with a multiscale grid- nesting assimilation framework, typically using a combination of these two approaches (Deng et al., 2009; Rogers et al., 2013). FDDA (Deng et al., 2009) was used in this research with the same strategy as used in Rogers et al. (2013). Both analysis nudging and observation nudging were applied on the 9 km grid, and only observation nudging was applied on the 3 km grid. In addition to assimilating observations and using the North America Regional Reanalysis model as initial conditions, we reinitialize the WRF model every 5 days, allowing 12 h of overlap period in consideration of model spin-up period to prevent model errors from growing over long periods. The observation data types assimilated include standard WMO surface and upper-air observations distributed by the National Weather Service (NWS), available hourly for the surface and 12-hourly for upper air, and the Aircraft Communications Addressing and Reporting System (ACARS) commercial aircraft observations, available anywhere in space and time with low-level observations near the major airports. The WRF model used in this study enables the chemical transport option within the model, allowing for the projection of CH_4 concentrations throughout the domain. Surface CH_4 emissions used as input for the model come from our CH_4 emissions inventory and are all contained within the 3 km nested grid. Each source of CH4 within our inventory is defined with its own tracer, allowing for the tracking of each individual source's contribution to the overall projected CH_4 enhancement within the model. For this study, CH_4 is treated as an inert gas. The potential for interaction with the hydroxyl radical (OH), the main sink of CH_4, is neglected. A calculation assuming an above-average OH mole fraction over a rural region of 0.5 pptv (Stone et al., 2012) and a reaction rate of 6.5 × 10−15 (Overend et al., 1975) produces a CH_4 sink of 0.5 ppb.h^{-1}. The duration of a flight can be up to 3 h, leading to a potential loss of 1.5 ppb over the course of a flight. This loss is small but not insignificant. CH_4 plumes associated with natural gas during each flight ranged between 15 and 70 ppb, and a change of 1.5 ppb could theoretically impact observations by as much as 10 % of the plume signal. However, this decrease in the CH_4 mole fraction would likely have equal impacts on both the background CH_4 values as well as the enhancement. Because emission calculations are based on the relative difference between the CH_4 background mole fraction and the enhancement downwind, it would take a gradient in the oxidation of OH to impact the results. Considering this relatively low destruction rate, the expected homogeneity of the sink across the region, and the difficulties associated with the simulation of chemical loss processes, we assumed that the CH_4 mass is conserved throughout the afternoon and therefore we ignored the impact of oxidation by OH.

Model optimization methodology

The objective of the model optimization technique is to solve for an emission rate as a percent of natural gas production that creates the best match between modelled CH_4 concentration maps, provided by the transport model, with actual CH4 mole fraction observations provided by the aircraft data. The optimization process in this study was originally designed to solve for natural gas emission from unconventional wells and emissions from compressor facilities separately. Because the flow rate of natural gas being processed was not avail- able for each compressor station, emissions at each facility were originally scaled based on the size of the station. However, when running the transport model using this emissions map, enhancements from the compressor stations produced plume structures nearly identical in shape to enhancements from the unconventional wells due to the similar spatial distributions of these two tracers. Without distinct differences between the enhancement patterns from each tracer, it becomes impossible to distinguish which emissions source must be adjusted to obtain the closest match to the observations. For this reason, emissions from compressor facilities are merged with unconventional well emissions in the optimized emission rate. Though the emission rate solved for in this experiment only uses the locations and production for the unconventional wells, this optimized rate represents emissions from both the wells and compressor facilities and are referred to as the modelled upstream natural gas emission rate. Midstream and downstream natural gas processes (such as processing, transmission and distribution of the gas) and emissions from conventional wells are not solved for in this study due to their minimal contribution (less than 5 %) to CH4 emissions in the region encompassed by the aircraft campaign.

Using the transport model WRF-Chem, CH_4 atmospheric enhancements were generated for each flight using different tracers to track different components to the overall CH_4 enhancement (e.g. animals/animal waste, distribution sector, industries). From these concentration fields, the upstream natural gas emission rate was solved for each flight using a three-step model optimization technique. First, a background concentration was determined for each flight and subtracted from the observations to create a set of "observed CH_4 enhancements", using

$$XEnhO = XObs - Xbg, \quad (1)$$

where XObs is the CH_4 mole fraction observation from the aircraft, Xbg is a chosen background value for the flight, and XEnhO is the calculated CH_4 enhancement at each observation. In this study, the background value is defined as the ambient CH_4 mole fraction over the region not accounted for by any of the sources within the model, with each flight having a unique background value. Box-pattern flights containing 2 loops around the basin may have a different background value assigned for each loop. To determine the background mole fraction, we start with the value of the observed mole fraction in the lowest 2^{nd} percentile of all observations within the boundary layer for a given flight or loop. This chosen background value represents the CH_4 mole fraction across the flight path from sources that are outside of our model domain. Because the background value is meant to represent the CH_4 mole fraction outside the model domain that is otherwise unaccounted for in our model, using the observations with the lowest CH_4 mole fraction is not always a sufficient definition for the background. On certain days, CH_4 enhancements from sources within the model domain can form plumes with wide spatial coverage that cover all observations during a flight. For example, during a flight the lowest CH_4 observations from the aircraft may be 1850 ppb, but the model simulation during that period indicates that all observations within the flight are being impacted by at minimum a 20 ppb enhancement. In this case, we would set our background value for the flight at 1830 ppb, and say that our 1850 ppb observations from the flight are a combination of an 1830 ppb background in addition to a 20 ppb enhancement from sources within the model. By subtracting this background value from our observations, we create a set of observed CH_4 enhancements, which can be directly compared to the model-projected enhancements.

The next step is to remove enhancements from this set that are not associated with emissions from upstream natural gas using

$XGasO = XEnhO - XOtherM, \quad (2)$

where XOtherM is the modelled CH_4 enhancement at each observation from sources unrelated to upstream natural gas processes, and XGasO is the observation-derived CH_4 enhancement associated with upstream natural gas emissions for each observation. In this step, each observed CH_4 enhancement has subtracted from it the projected non-natural gas enhancement from the model (i.e. nearest grid point in space) using the corresponding model output time closest to the observation within a 20 min time interval. This creates a set of observed CH_4 enhancements related only to emissions from upstream gas processes, filtering out potential signals from other CH_4 emitters and providing a set of observed enhancements that can be directly compared to the projected upstream natural gas enhancement within the model. By subtracting these other sources from the observations, we make the assumptions that our emissions inventory is accurate for non-natural gas sources and that the transport of these emissions is perfect, both of which are actually uncertain. Because errors exist in both the emissions and transport, it is possible to create a negative observation-derived upstream gas enhancement if model-projected enhancements from other sources are larger than the observation-derived enhancement. From the 10 flights, 16 % of the observation- derived enhancements are negative, but only 3 % are negative by more than 5 ppb. To avoid solving for unrealistic negative values, these negative observation-based upstream gas enhancements are set to 0. Errors associated with this issue and other uncertainties with our inventory are examined further in the uncertainly analysis section of this paper.

In the final step, the upstream natural gas emission rate within the model is adjusted to create the best match between the modelled upstream gas enhancement and observation- derived upstream gas enhancement using

$J = XGasO - C \cdot XGasM, \quad (3)$

where XGasO and XGasM are the observed and modelled enhancements for each observation. In this equation, J is a cost function we are trying to minimize by solving for a scalar multiplier C, which, when applied to the modelled natural gas enhancements, creates the smallest sum of the differences between the observation-derived upstream gas enhancement and the modelled upstream enhancement.

Model evaluation

Table 1 shows the wind speed and boundary layer height errors for each flight as well as the optimized and corrected natural gas emission rates. On days where model performance was poor with regards to the wind speed and boundary layer height, we can see changes in the corrected emission rate. For most days, this change is less than 20 % different than the original optimized emission rate. However, both 14 and 25 May have corrected emission rates which are around a factor of 2 different from their original value. Whether these corrected emission rates are more accurate than the original optimized rates is debatable. To calculate these alternative emission rates, we must assume that the wind speeds and boundary layer heights from our limited number of observations are the true values in the atmosphere, which may not be the case. Regardless of which rate is more accurate for each flight, the overall 16 % high bias in the model wind speed and the 12 % low bias in the model boundary layer result in compensating errors that cancel out, and the mean emission rates across all flights end up similar. Thus, any errors associated with these two meteorological variables has a trivial impact on the overall calculated emission rate for the region, and the uncorrected emission rates are used for the final mean and uncertainty calculations.

The largest uncertainty exists for the 22 May flight, where an unexplained enhancement along the northern transect led to a poor match between the modelled enhancements and the observed enhancements. This may ex- plain the anomalously high optimized emission rate for that day. Other flights with large uncertainty are those that occurred on 24 May, where enhancements from south-western PA are believed to be influencing large portions of the observations. Based on the conservative methodology used to calculate these uncertainties, we assume the total uncertainty for each flight represents a 2σ range of possible emission rates

and calculate a weighted mean and a 2σ confidence interval for the overall upstream emission rate across the 10 flights. From this approach, we find a mean upstream emission rate of 0.36 % of production and a 2σ confidence interval from 0.27 to 0.45 % of production.

Day	Optimized NG (% of production)	Wind error	Boundary error	Corrected NG emission rate (% of production)
14 May	0.37	31 %	−33 %	0.80
21 May	0.53	3 %	39 %	0.37
22 May	1.15	37 %	−18 %	1.02
23 May	0.45	34 %	9 %	0.37
24 May	0.68	48 %	−21 %	0.58
24 May	0.36	48 %	−21 %	0.30
25 May	0.99	3 %	−43 %	1.69
28 May	0.33	−4 %	−8 %	0.37
29 May	0.35	4 %	1 %	0.33
3 June	0.26	19 %	−8 %	0.24
Average	0.55	16 %	12 %	0.61

Table 1: Optimized natural gas emission rates for each flight as well as corrected emission rates adjusting for errors in the model wind speed and boundary layer height. For wind speed and boundary layer height error, a negative value represents a model value lower than the observations.

GRAPHICAL MATERIALS LIST

Figure 1: four tower locations instrumented during the project. The South tower (S) and North tower (N) provided background concentrations while Central (C) and East (E) towers measured the enhanced concentrations of CH_4 from the unconventional gas production area.

Figure 2: Field sampling flow schematic with automatic calibration system using four gas-phase standards of unique isotopic $^{13}CH_4$ values (δ) and CH_4 (X) mixing ratios at ambient (amb) and heavy and high (HI) and low (Lo1, Lo2) mixing ratios, respectively.

Figure 3. Low tank methane isotopic ratio differences from known value, for the individual calibration cycles, and for 1-, 5-, and 10-day means, for the South tower for September - December 2016. An improved calibration tank sampling strategy was implemented on 3 December 2016. The low tank is independent of the isotopic ratio calibration.

Figure 4**:** Atmospheric CH_4 mixing ratios in ppb collected at the four instrumented towers during the course of the project. Data are available at http://dx.doi.org/10.18113/D3SG6N.

Figure 5: Probability distribution function of isotopic ratio enhancement above the background South tower for the A) North, D) Central, and G) East towers for afternoon hours (1700–2059 UTC, 1200–1559 LST). The time scale of the individual data points for all plots is 10 min and the time period is January – May 2016. The bin size for A), D)

and G) is 0.2 ‰. Probability distribution function of methane mole fraction enhancements for the B) North, E) Central, and H) East towers. Note that the scale for B), E, and H) has been truncated to focus on majority of the data points. The bin size is 10 ppb CH_4. Keeling plots for the C) North, F) Central, and I) East towers. The black box in each plot indicates the approximate scale of the corresponding isotopic ratio enhancement and methane mole fraction enhancement plots.

Figure 6: Keeling plots for the Central tower for the eight largest peak in the non-afternoon methane time series. Black lines indicate the best-fit lines. Correlation coefficients (r^2), day of year (DOY) and y-intercepts are indicated in the plots.

Figure 7: Calculated upstream natural gas emission rates using (black) model optimization technique and (red) aircraft mass balance technique. Error bars represent the 2σ confidence interval for each flight. Mass balance performed in Peischl et al. (2015) included for comparison.

Figure 8: Measured CH_4 vs. C_2H_6 observations from the late-afternoon flight on May 24th, 2015 corresponding to elevated CH_4-to-C_2H_6 ratios from SW PA. Coal mines and wet gas wells present larger values than dry gas from NE PA, therefore confirming the presence of other sources due to long distance transport.

Figure 9: Diagram of the different flux sub-regions used in the inversion. Towers (green pins) and wells (pink dots) are plotted overtop

Figure 10: Map of the percent change in the posterior flux compared to the prior flux using tower observations from Oct-Dec 2015.

Figure 11: Observed CH_4 mole fractions at each of the four tower locations from September 2015 to September 2016.

Figure 12: a.) Number of hourly intervals in which each tower recorded the largest CH_4 mole fraction compared to all other towers. b.) Same as a. but using only hourly periods where the mean wind direction had a southerly component. c.) Same as a. but using only hourly periods where the mean wind direction had a northerly component.

Figure 13: Average influence functions calculated at East tower for hours when East tower recorded the (left) highest CH_4 observation, and (center) lowest CH_4 observation among all four towers. (right) A map showing the subtraction of the center figure from the left figure. Warmer colors in this figure illustrate footprints which correspond with periods when East tower observes its highest CH_4 concentrations, whereas cooler coolers are common footprints on periods where East tower records its lowest CH_4 concentrations compared to other towers.

Figure 14**:** Atmospheric CH_4 mixing ratio enhancements (in ppm) measured across the tower network from May 2015 to January 2017.

REFERENCES

Barkley, Z. R., Lauvaux, T., Davis, K. J., Deng, A., Miles, N. L., Richardson, S. J., Cao, Y., Sweeney, C., Karion, A., Smith, M., Kort, E. A., Schwietzke, S., Murphy, T., Cervone, G., Martins, D., and Maasakkers, J. D.: Quantifying

methane emissions from natural gas production in north-eastern Pennsylvania, Atmos. Chem. Phys., 17, 13941-13966, https://doi.org/10.5194/acp-17-13941-2017, 2017.

Conway, T. & Tans, P. Trends in atmospheric carbon dioxide. http://www.esrl.noaa.gov/gmd/ccgg/trends (2011).

GAW Report No. 213, 2014. 17th WMO/IAEA Meeting on Carbon Dioxide, Other Greenhouse Gases and Related Tracers Measurement Techniques (GGMT-2013), Beijing, China, 10–13 June 2013).

Kort, E. A., M. L. Smith, L. T. Murray, A. Gvakharia, A. R. Brandt, J. Peischl, T. B. Ryerson, C. Sweeney, and K. Travis (2016), Fugitive emissions from the Bakken shale illustrate role of shale production in global ethane shift, Geophys. Res. Lett., 43, 4617–4623, doi:10.1002/2016GL068703.

Langlois, L. A., Drohan, P. J., and Brittingham, M. C.: Linear infrastructure drives habitat conversion and forest frag- mentation associated with Marcellus shale gas development in a forested landscape, J. Environ. Manage., 197, 167–176, https://doi.org/10.1016/j.jenvman.2017.03.0452017.

Maasakkers, J. D., Jacob, D. J., Sulprizio, M. P., Turner, A. J., Weitz, M., Wirth, T., Hight, C., DeFigueiredo, M., Desai, M., Schmeltz, R., Hockstad, L., Bloom, A. A., Bowman, K. W., Jeong, S., and Fischer, M. L.: Gridded National Inventory of U.S. Methane Emissions, Environ. Sci. Technol., 50, 13123–13133, https://doi.org/10.1021/acs.est.6b02878, 2016.

Marchese, A. J., Vaughn, T. L., Zimmerle, D. J., Martinez, D. M., Williams, L. L., Robinson, A. L., Mitchell, A. L., Subramanian, R., Tkacik, D. S., Roscioli, J. R., and Herndon, S. C.: Methane Emissions from United States Natural Gas Gathering and Processing, Environ. Sci. Technol., 49, 10718–10727, https://doi.org/10.1021/acs.est.5b02275, 2015.

Miles, N. L., Martins, D. K., Richardson, S. J., Rella, C. W., Arata, C., Lauvaux, T., Davis, K. J., Barkley, Z. R., McKain, K., and Sweeney, C.: Calibration and Field Testing of Cavity Ring-Down Laser Spectrometers Measuring CH4, CO2, and δ13CH4 Deployed on Towers in the Marcellus Shale Region, Atmos. Meas. Tech. Discuss., https://doi.org/10.5194/amt-2017-364, in review, 2017.

Montzka, S. A., Myers, R. C., Butler, J. H. and Elkins, J. W. (1994), Early trends in the global tropospheric abundance of hydrochlorofluorocarbon-141b and 142b. Geophys. Res. Lett., 21: 2483–2486. doi:10.1029/94GL02342

Omara, M., Sullivan, M. R., Li, X., Subramanian, R., Robinson, A. L., and Presto, A. A.: Methane Emissions from Conventional and Unconventional Natural Gas Production Sites in the Marcellus Shale Basin, Environ. Sci. Technol., 50, 2099–2107, https://doi.org/10.1021/acs.est.5b05503, 2016.

Peischl, J., Ryerson, T. B., Aikin, K. C., de Gouw, J. A., Gilman, J. B., Holloway, J. S., Lerner, B. M., Nadkarni, R., Neuman, J. A., Nowak, J. B., Trainer, M., Warneke, C., and Parrish, D. D.: Quantifying atmospheric methane emissions from the Haynesville, Fayetteville, and northeastern Marcellus shale gas production regions, J. Geophys. Res.-Atmos., 120, 2119–2139, https://doi.org/10.1002/2014jd022697, 2015

Rella, C. W., Hoffnagle, J., He, Y., and Tajima, S.: Local- and regional-scale measurements of CH4, δ13CH4, and C2H6 in the Uintah Basin using a mobile stable isotope analyzer, Atmos. Meas. Tech., 8, 4539-4559, doi:10.5194/amt-8-4539-2015, 2015.

Stein AF, Draxler RR, Rolph GD, Stunder BJB, Cohen MD, Ngan F (2015) NOAA's HYSPLIT Atmospheric Transpport and Dispersion Modeling System, Bulletin of the American Meteorological Society: 2059-2077.

Turnbull J, Guenther D, Karion A, Sweeney C, Anderson E, Andrews A, Kofler J, Miles N, Newberger T, Richardson S, Tans P (2012) An integrated flask sample collection system for greenhouse gas measurements, Atmospheric Measurement Techniques 5: 2321-2327.

Zavala-Araiza, D., Alvarez, R. A., Lyon, D. R., Allen, D. T., Marchese, A. J., Zimmerle, D. J., and Hamburg, S. P.: Super-emitters in natural gas infrastructure are caused by abnormal process conditions, Nat. Commun., 8, 14012, https://doi.org/10.1038/ncomms14012, 2017.

Zimmerle, D. J., Williams, L. L., Vaughn, T. L., Quinn, C., Subramanian, R., Duggan, G. P., Willson, B., Opsomer, J. D., Marchese, A. J., Martinez, D. M., and Robinson, A. L.: Methane Emissions from the Natural Gas Transmission and Storage System in the United States, Environ. Sci. Technol., 49, 9374–383, https://doi.org/10.1021/acs.est.5b01669, 2015.

LIST OF ACRONYMS AND ABBREVIATIONS

CRDS: Cavity Rind-Down Spectroscopy
GPS: Global Positioning System
LPDM: Lagrangian Particle Dispersion Model
NOAA: National Oceanic and Atmospheric Administration
PA: Pennsylvania
PFP: Portable Flask Package
WRF: Weather Research and Forecasting model